INVESTIGATION OF A GENERIC WARHEAD CONTAINING PLASTIC BONDED EXPLOSIVE UNDER LIQUID FUEL FIRE BY NUMERICAL AND TEST METHODS

A THESIS SUBMITTED TO
THE GRADUATE SCHOOL OF NATURAL AND APPLIED SCIENCES
OF
MIDDLE EAST TECHNICAL UNIVERSITY

BY

HAKAN ŞAHİN

IN PARTIAL FULLFILLMENT OF THE REQUIREMENTS
FOR
THE DEGREE OF MASTER OF SCIENCE
IN
AEROSPACE ENGINEERING

DECEMBER 2015

Approval of thesis:

INVESTIGATION OF A GENERIC WARHEAD CONTAINING PLASTIC BONDED EXPLOSIVE UNDER LIQUID FUEL FIRE BY NUMERICAL AND TEST METHODS

submitted by **HAKAN ŞAHİN** in partial fulfillment of the requirements for the degree of **Master of Science in Aerospace Engineering Department, Middle East Technical University** by,

Prof. Dr. Gülbin Dural Ünver
Dean, Graduate School of **Natural and Applied Sciences** _____

Prof. Dr. Ozan Tekinalp
Head of Department, **Aerospace Engineering** _____

Assoc. Prof. Dr. Dilek Funda Kurtuluş
Supervisor, **Aerospace Engineering Dep., METU** _____

Dr. Bekir Narin
Co-Supervisor, **TÜBİTAK SAGE** _____

Examining Committee Members:

Prof. Dr. İsmail H. Tuncer
Aerospace Engineering Dep., METU _____

Assoc. Prof. Dr. Dilek Funda Kurtuluş
Aerospace Engineering Dep., METU _____

Prof. Dr. Yusuf Özyörük
Aerospace Engineering Dep., METU _____

Assoc. Prof. Dr. Sinan Eyi
Aerospace Engineering Dep., METU _____

Assist. Prof. Dr. Sıtkı USLU
Mechanical Engineering Dep.,
TOBB University of Economics and Technology _____

Date: 29 December, 2015

I hereby declare that all information in this document has been obtained and presented in accordance with academic rules and ethical conduct. I also declare that, as required by these rules and conduct, I have fully cited and referenced all material and results that are not original to this work.

Name, Last Name : Hakan ŞAHİN

Signature :

ABSTRACT

INVESTIGATION OF A GENERIC WARHEAD CONTAINING PLASTIC BONDED EXPLOSIVE UNDER LIQUID FUEL FIRE BY NUMERICAL AND TEST METHODS

Şahin, Hakan
M.S., Department of Aerospace Engineering
Supervisor : Assoc. Prof. Dr. Dilek Funda Kurtuluş
Co-Supervisor : Dr. Bekir Narin

December 2015, 78 pages

The present work provides a design methodology for a munition against fast cook-off threat for type V insensitivity requirement. The experimental and numerical results for a generic test item (warhead) filled with a PBXN-109 explosive are presented.

Two key points for the design of an insensitive munition against fast cook-off threat, which are time to reaction and critical vent area is studied. Dividing the problem as pre-ignition and post- ignition will allow one to manage this complex problem to handle easier than its original form.

The first part of the study covers 2-D and 3-D simulations of the problem by modeling the generic test item geometry by commercial CFD software (ANSYS - Fluent). The second part of the study reveals low pressure (2-10 MPa) burn characteristics of a PBXN-109 by strand burner tests. After obtaining pressure dependent burning rate, conservation of mass equation is used to determine the chamber pressure using MATLAB Simulink software.

Calculations are compared with the tests performed. Results are seen to be in reasonable agreement with some discrepancies at 8.9% for time to reaction prediction and at 10.9% for ventilation characteristics analyses. Possible reasons of these differences are discussed in this study.

Keywords: Insensitive Munition, Fast Cook-Off, Time-To-Reaction, Strand Burner Test, PBXN-109

ÖZ

SIVI YAKIT YANGININA MARUZ KALAN PLASTİK PATLAYICI İÇERİKLİ BİR HARP BAŞLIĞININ NÜMERİK VE TEST METODUYLA İNCELENMESİ

Şahin, Hakan
Yüksek Lisans, Havacılık ve Uzay Mühendisliği
Tez Yöneticisi : Doç. Dr. Dilek Funda Kurtuluş
Ortak Tez Yöneticisi : Dr. Bekir Narin

Aralık 2015, 78 sayfa

Yapılan bu çalışmada sıvı yakıt yangını tehdidine karşı tip V duyarsızlık isterine sahip bir mühimmatın tasarımına yönelik bir metodolojisi sunulmuştur. PBXN-109 patlayıcısı içeren test kalemi (harp başlığı) ile yapılan deneysel ve nümerik sonuçlar paylaşılmıştır.

Reaksiyon başlangıç zamanı ve kritik tahliye deliği çapı, sıvı yakıt yangınına karşı tasarımı yapılan bir mühimmat için iki önemli anahtar parametredir. Problemin reaksiyon öncesi ve sonrası olarak ikiye bölünmesi bu kompleks problemin çözümü için tasarımcıya kolaylık sağlayabilir.

Çalışmanın ilk aşaması test kaleminin 2 ve 3 boyutlu olarak ticari hesaplamalı akışkanlar dinamiği programı ANSYS-Fluent ile modellenmesini içermektedir. İkinci aşama ise PBXN-109 patlayıcısına ait düşük basınçlı (2-10MPa) yanma karakteristiğinin strand burn testleri ile çıkarıldığı çalışmayı içermektedir. Basınca bağlı yanma hızının elde edilmesi ile birlikte test kalemi içerisinde oluşacak basıncın tespiti için MATLAB Simulink ticari yazılımında kütlenin korunumu denklemleri kullanılmıştır.

Hesaplamalar yapılan testler ile karşılaştırılmıştır. Buna göre, sonuçlar makul kabul edilebilecek seviye birbiri ile örtüşmekte olup; reaksiyonun süresinin tespiti için yapılan öngörüler için %8,9 olup, kritik tahliye deliğinin tespiti için yapılan

çözümlemeler için %10,9'dur. Bu farklara olması muhtemel sebepler çalışma içerisinde paylaşılmıştır.

Anahtar Kelimeler: Duyarsız Mühimmat, Sıvı Yakıt Yangını, Reaksiyon Süresi, Yanma Hızı Testleri, PBXN-109

To My Family

ACKNOWLEDGEMENTS

I would like to express my deepest thanks and appreciation to my supervisor, Assoc. Prof. Dr. Dilek Funda KURTULUŞ, for her supervision and continuous support during all stages of this thesis.

I would like to give my special appreciations to the Chief of the Terminal Ballistics and Fuze Technologies Division at TÜBİTAK SAGE, Dr. Bekir NARİN for initiating this thesis and encouragement on my studies.

I would like to express my sincere appreciation to Mr. Başar ESİRGEN for his crucial advices and invaluable efforts during the preparation of this thesis.

My special thanks also go to my colleagues at TÜBİTAK SAGE, Mr. Oğuzhan AYISIT, Mr. Tahir TURGUT, Mr. Salih SARAN and Mr. Fatih CENGİZ for their discussion on the subject.

Finally, the greatest thanks go to my parents and lovely wife who supported and encouraged me throughout my whole life. It would be impossible without their patience and understanding.

TABLE OF CONTENTS

LIST OF TABLES

TABLES

LIST OF FIGURES

FIGURES

LIST OF SYMBOLS

a	burn rate coefficient
A	molar fraction
A_{vent}	ventilation area, m^2
A_{burn}	total burn surface area, m^2
c_p	specific heat capacity, *J/kg/K, Cal/g/K*
C_D	discharge coefficient
E	activation energy, *J/kg/K*
k	specific heat ratio
k_1, *k2, k3*	chemical reaction kinetic model step
L/D	length over diameter
M	Mach number
$\dot{m}$	mass flux
n	burning rate pressure exponent
u^*	particle velocity at throat, *m/s*
P	pressure, *MPa*
P^*	pressure at throat, *MPa*
R	universal gas constant, *J/mol/K*
r_{burn}	explosive burn rate, *m/s, mm/sn*
S	rate of chemical heat production, *J/s*
Q_{act}	heat of reaction, *J/kg*
t	time, *s*
T	temperature, *K*
T^*	temperature at throat, *K*
V	volume, m^3
Z	frequency factor, *1/s*

Greek Symbols

λ	thermal conductivity, *J/m/s/K*
ρ	density, kg/m^3
ρ^*	density at throat, kg/m^3

LIST OF ABBREVIATIONS

IM	Insensitive Munition
PBXN	Plastic Bonded Explosive
TtR	Time to Reaction
TÜBİTAK	Türkiye Bilimsel ve Teknolojik Araştırma Kurumu
SAGE	Savunma Sanayi Araştırma Geliştirme Enstitüsü
TNT	Trinitrotoluene
STANAG	Standardization Agreement of NATO
HMX	Octahydrotetranitrotetrazine
RDX	Cyclotrimethylenetrinitramine
DDT	Deflagration to Detonation Transition

CHAPTER 1

INTRODUCTION

Energetic materials such as explosives, pyrotechnics and propellants are widely used in many military applications. Explosives are defined as materials which react to produce a violent expansion of hot gas, an explosion, which rapidly delivers energy to its surroundings. The rate of transformation from solid to hot gas takes place on timescales of microseconds. Propellants are less violent in reaction and are used to accelerate objects such as missiles and bullets. For propellants transformation takes place in a slower timescale which is milliseconds. Pyrotechnics are systems which react to produce an effect such as smoke, light or noise with reaction times from milliseconds to many minutes [1].

Comparing energetics materials with other materials such as petrol, petrol contains six times more available energy as the same mass of TNT but unlike petrol, TNT releases its energy a hundred million times faster [1]. These reaction (transformation) time form the basis of the explosion.

Today, safety design of the munitions against unplanned stimuli like terrorist attack, accidental fire environment etc. becomes as important as the design for performance and operational requirements. Many nations have been undertaken significant work to reduce the response of munition systems under attack. These efforts include understanding explosive response under thermal load and mechanical shocks. Knowing the material behavior of the explosive, it becomes possible to prevent unwanted reaction of the munition while it is in non-operational condition by taking precautions at the design phase.

Several studies have been performed in TÜBİTAK-SAGE for the design of munition components like warheads and rocket motors against threats especially after insensitivity became a requirement by the Turkish Ministry of Defense. Liquid fuel fire is one of the threads that munition can be exposed to. Past studies that have been

made includes test of munitions having a case material that can melt and allow explosive to have a contact with atmosphere directly. But not all munitions can take advantage of the same solution such as munitions that have a penetrator type of warhead.

In this thesis study, investigation of behavior of the warhead under liquid fuel fire is performed by using analytical formulas, commercial Fluent program and performing tests. It is aimed to develop a general method for designing insensitive munitions against liquid fuel fire threat and minimize the test number required in the test phase.

1.1. Definition of Insensitive Munitions, Threats and Reaction Levels

Insensitive munition by the definition of STANAG 4439 is: "…munitions which reliably fulfil their performance, readiness and operational requirements on demand but which minimize the probability of inadvertent initiation and severity of subsequent collateral damage to weapon platforms, logistic systems and personnel when subjected to unplanned stimuli…" [2]. These unplanned stimuli are stated as follow:

- Fast heating (fast cook-off)
- Slow heating (slow cook-off)
- Bullet impact
- Fragment impact
- Shaped charge jet impact
- Sympathetic reaction

In Figure 1, possible threats against munitions, related insensitive munitions tests and phenomena are shown schematically [3].

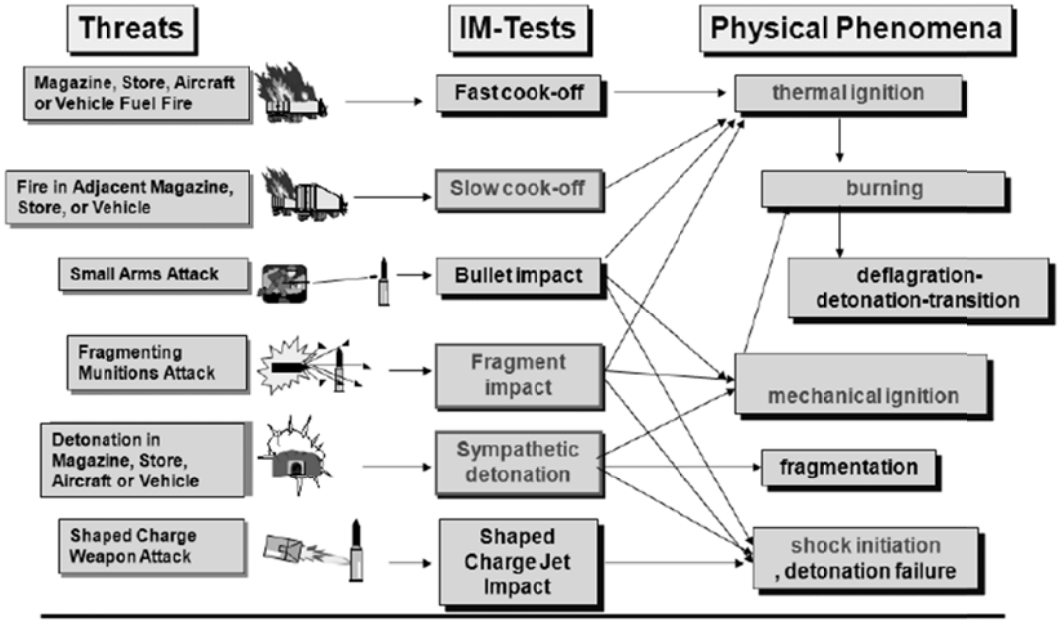

Figure 1. Threats against Munitions, Related Insensitive Munitions Test and Phenomena [3]

There are different reaction types that munitions react under the effect of these stimuli and classified under 6 types which are [4]:

- **Detonation (Type I):** The most violent type of munition reaction where the energetic material is consumed in a supersonic decomposition.
- **Partial Detonation (Type II):** The second most violent type of munition reaction where some energetic material is consumed in a supersonic decomposition.
- **Explosion (Type III):** The third most violent type of munition reaction with sub-sonic decomposition of energetic material and extensive fragmentation.
- **Deflagration (Type IV):** The fourth most violent type of munition reaction with ignition and burning of confined energetic materials which leads to a less violent pressure release.

- **Burn (Type V):** The fifth most violent type of munition reaction where the energetic material ignites and burns non-propulsive.

- **No-reaction (Type VI):** The least violent type of munition response where any reaction is self-extinguished immediately upon removal of the external stimulus.

In Figure 2 the reaction types to accidental stimuli that are explained above are shown schematically [5].

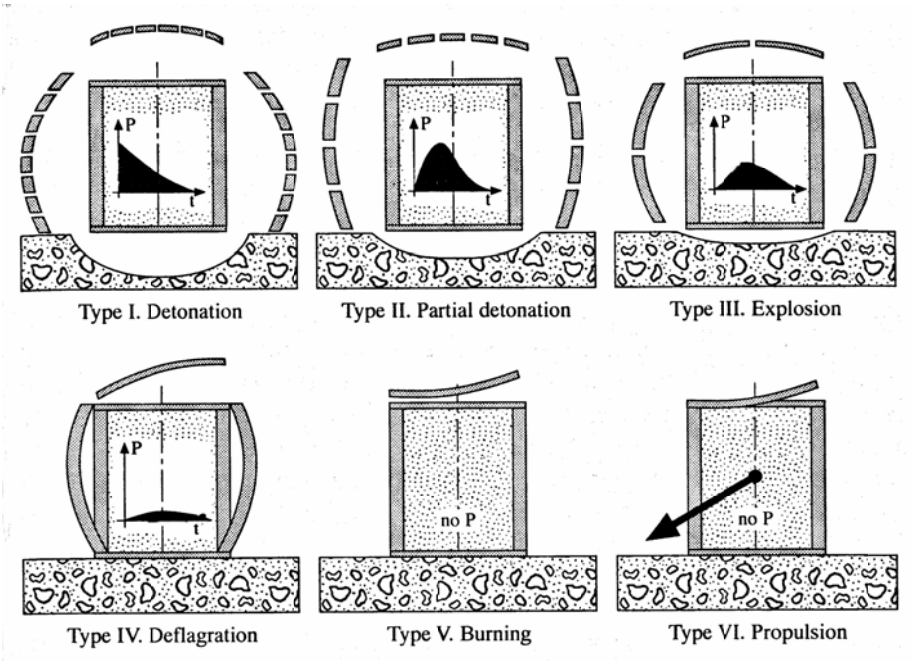

Figure 2. Reaction Types of Munitions to Accidental Stimuli [5]

1.2. Historical Background

History is replete with accidents and incidents that involved or were caused by the unintended functioning or reaction of munitions, which resulted in hazardous consequences to the owning or using forces and Nation. Forrestal accident in 1967 and Camp Doha accident in 1991 are two of the well-known disasters with large amount of personnel and equipment losses.

In July 1967, USS Forrestal, a USS Naval aircraft carrier which is shown in Figure 3 was conducting combat operations in the waters near Vietnam [6].

Figure 3. USS Forrestal before the Accident [6]

During preparations for a combat sortie, a forward firing unguided rocket flew across the deck of the carrier which was loaded with planes fully fuelled and armed. The missile struck another plane causing external fuel tank of the airplane to spill and igniting the fuel which is known as JP-5. Flowing burning fuel then engulfed additional planes and caused an M-117 bomb to explode. This has caused more fuel tanks to spill and ignite and more bombs and several missile warheads to explode. These actions and reactions resulted in 134 deaths, 161 injuries, 21 aircraft destroyed, 39 aircraft damaged and the ship removed from combat actions [6]. In Figure 4, a photo of sailors attempting to fight fires during the incident is shown [7].

Figure 4. Forrestal Aircraft Carrier Accident, 1967 [7]

Figure 5 shows the operational impact of IM and non-IM bombs to an aircraft career. It is obvious that if the munitions existed on the deck had had the insensitive munitions characteristics, the amount of total loss could have been reduced dramatically [8].

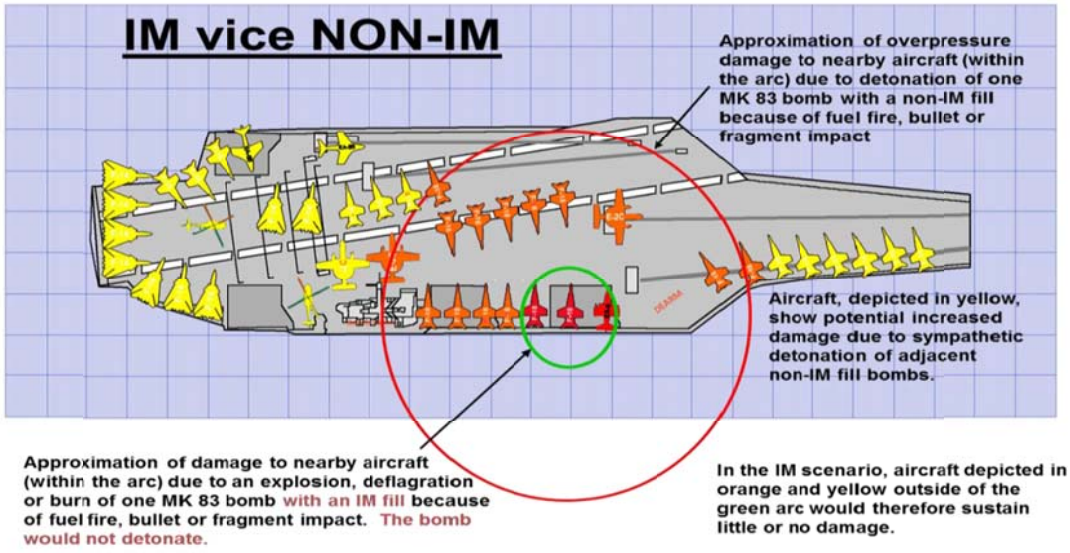

Figure 5. IM and non-IM Munition Accidental Causality Approximation [8]

Camp Doha accident which occurred in Kuwait 1991 and its effect to multiple tanks and armored personal carriers is shown in Figure 6. This incident is known to be initiated by internally stored non-IM munitions that are subjected to single vehicle engine fire. It is resulted in 3 deaths, 52 injuries and 150 vehicle destroyed [9].

Figure 6. Camp Doha Accident, 1991 [9]

Developing and introducing insensitive munitions systems in the operational area reduces the life losses and operational costs. Many analyses have been performed by the researchers about the outcomes of implementing insensitive munitions policies. Researchers have mentioned about the benefits and the future trends in the insensitive munitions concept [10], [11], [12].

The IM technology objectives are to increase total life cycle safety, increased platform and crew survivability, increase operation safety, reduced weapon life cycle costs, facilitate reduction in hazard classification through increased storage safety which facilitates reduced quantity-distance requirements.

In this study among all other threats, main concern is focused on the fast cook-off threat. In fast cook-off test munitions are subjected to a heat source in order to simulate liquid fuel fire accidental condition. The purpose of the fast cook-off test is to record the test item response due to a rapid increase in temperature. An aircraft

fuel fire with an average steady-state temperature of at least 800 °C is used as the test stimulus [4].

1.3. Literature Survey

Thermal Initiation Theory describes the initiation of deflagration due to thermal effects from surrounding conditions and the heat generated inside the energetic material. Understanding the ignition characteristics of energetic materials is the basis of the studies in order to predict the cook-off behavior of munitions and development of design techniques for insensitive munitions.

Energetic materials are unstable and decompose rapidly as their temperature is raised. Energetic materials can be characterized by an ignition temperature; however, the temperature at which ignition occurs more accurately depends upon the geometry of the energetic material and the rate at which it is heated [13].

Energetic materials exothermically decompose when exposed to external heat source. A part of the heat release accompanied with the decomposition is dissipated out while some is accumulated inside the energetic material. Any material that gives exothermic decomposition reactions during heating like explosive in a warhead, propellant in a rocket motor or even a bale of wool may end up with ignition. Self-heating can be defined as the increase of temperature of a material due to the heat generated inside with exothermic decomposition reactions [14]. Decomposition rate increases as the temperature increases, thus self-heating rate increases.

To determine whether the energetic material will undergo a thermal initiation under certain surrounding conditions, it is required to know the critical temperature of that material which is a function of the chemical, physical, and the geometrical properties of the material. Critical temperature is the limit surrounding temperature under which no ignition occurs regardless of the exposition time to that temperature. On the other hand, under a surrounding temperature conditions above the critical temperature, ignition eventually occurs and the level of temperature only affects time or location of ignition.

In Figure 7, the effect of heating rate on the location of ignition of an energetic material is visualized [14]. In all cases, energetic material is heated from surrounding boundary but with different heating rates. For the low heating rate cases, after a temperature limit, self-heating rate becomes more dominant over the heating rate by the surrounding. Because of the low conduction coefficient of solid explosive materials, the temperature of more isolated part of the explosive filling tends to increase most. This causes ignition point to be moved from the outer edges to places where explosive material density over the volume is large.

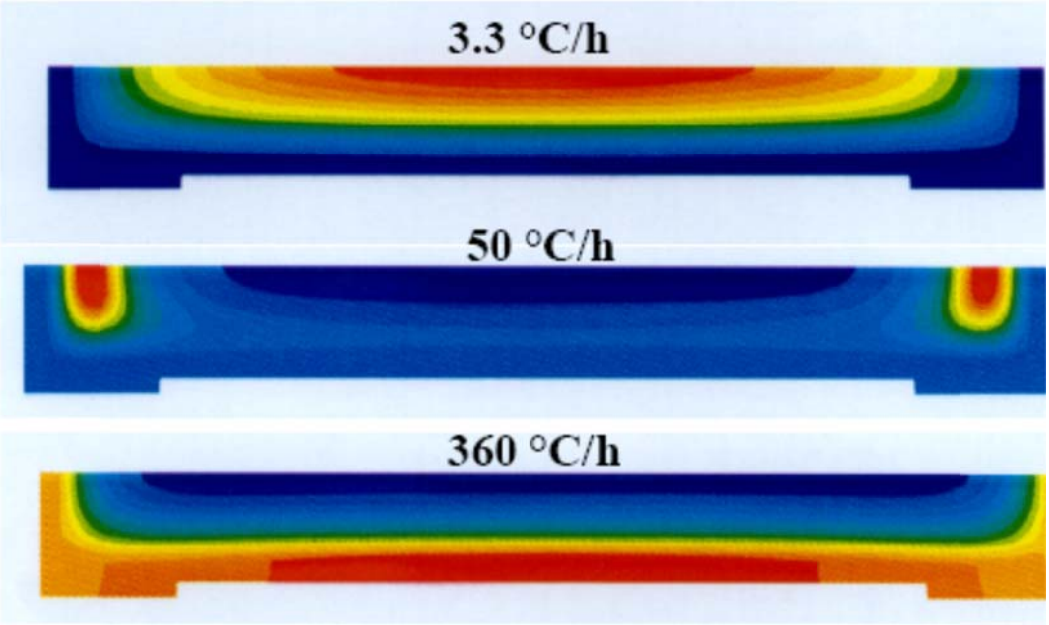

Figure 7. Temperature Profile Predictions at Ignition for an Energetic Material for Different Heating Rates [14]

Since fast cook-off is a case where the heating rate is very large (bigger than 600°C/h), critical temperature of the energetic material is independent from the geometry and ignition occurs on the edges close to boundaries where heating occurs.

Studies of thermal initiation of energetic materials start with Semenov [15]. Semenov made the uniform temperature distribution assumption in the energetic material with zero order reaction kinetics [15]. This was the origin of the thermal initiation studies. However, this theory was only applicable for systems like well stirred liquids. However, as the conduction coefficient of solid energetic materials are relatively low

and uniform temperature distribution assumption is not applicable, Frank-Kamenetskii [16] proposed a theory based on the conductive heat transfer in the energetic material which allows time dependent temperature distribution.

Numerical studies which is based on Frank-Kamenetskii's work on predicting the ignition times and temperatures for energetic materials have been performed starting from 1960's. Zinn and Mader [17] applied Fourier series spatial representation for the solution to the reactive heat conduction equation to obtain ignition times for explosive material. Merzhanov and Abramov [18] used finite difference method for one-dimensional reactive heat conduction with the zero-order kinetic model. Suceska [19] used finite difference method and developed code THERMEX for the solution of the reactive heat conduction equation problem with the zero-order kinetic model. Anderson [20] developed the code TEPLO using finite difference method, which took temperature dependent material properties into account. Isler and Kayser [21] and McGuire and Tarver [22] used different kinetic models instead of zero-order kinetic model such as power law kinetic model to predict the ignition behavior of different energetic materials. There are also some methods presented by Pakulak [23] and Victor [13] for predicting the time to reaction by using analytical equations to solve 1-D heat transfer. Victor has implemented these methods to excel spread sheets for determining internal temperatures by taking into account the self-heating of the explosive, however none of those studies were involved into a chemical reaction modelling code. Instead, all used simple kinetic models as stated above to estimate and implement heat generated by the explosive as it gets heated by the stimuli.

Other than those studies, Lawrence Livermore National Laboratory, a high explosive cook-off study has been conducted by a group of engineers and physicist to model the response of energetic materials to thermal stimuli and the processes involved in the energetic response [24], [25]. This study had coupled the two parts of the problem that was stated above which are pre-ignition and post-ignition. It is stated that several new algorithms have been developed to increase the accuracy and fidelity of the modeling process including a level set driven multi-material deflagration model, a multi-temperature mixed material treatment, self-consistent

thermal-hydro coupling, full implicit quasi-static hydrodynamics, ALE slide surfaces and ALE slide deletion.

On the other hand, ventilation of burn products might be vital for a system containing energetic material for unplanned thermal or mechanical stimuli. The question that is generally raised is “what is the required ventilation size for preventing system to react violently”.

Graham [26] and Victor [13] derived a methodology for the determination of critical ventilation requirements of rocket motor and warheads using the internal ballistics. They both assumed that the flow over the ventilation area becomes sonic, and simplified and derived equations of internal ballistics accordingly. Graham [26] also used ballistic analysis methodology for the determination of critical ventilation requirements of rocket motor.

1.4. Motivation and Objectives

Design phase of an insensitive warhead can be complex considering the number of tests which should be carried on. Considering the cost and environmental concerns, among all other insensitive munition sign tests, fast cook-off will probably lead in a "number of tests to be decreased" list for most IM design authorities.

This thesis study is related to the insensitive munition studies that are going on at TÜBİTAK SAGE Terminal Ballistics Division. The aim of the study is to have an improved knowledge on the theory behind the fast cook-off stimuli and have a methodology for being able to design a munition that has reduced impact on its surroundings. By doing so, this will allow us to decrease the number of tests on the design phase leading into the decrease of cost and negative environmental effects.

CHAPTER 2

METHOLODOGY

In IM design of a typical warhead against fast cook-off test, there are two important parameters to be predicted which are time to reaction (TtR) and critical ventilation area. TtR is important for the precautions that are taken to work before reaction occurs, whereas critical ventilation area is important for safe disposal of burn products of energetic materials. Dividing the problem as pre-ignition and post-ignition will allow one to manage this complex problem to handle easier than its original form.

Although the present methodology is valid for all energetic materials, PBXN-109 (64% RDX, 20% Al, 16% DOA/HTPB) is considered as the energetic material for the purpose of illustration and as it is widely used as the main charge for most warheads designed/manufactured worldwide. Although plastic-bonded explosives show relatively low responses to auxiliary thermal/mechanical effects, as long as they are exposed to heat within a closed chamber/casing any explosive, it will lead to deflagration to detonation transition unless necessary precautions are taken.

2.1. Pre-Ignition Phase: Thermal Initiation

The kinetic model to predict the thermal decomposition of a RDX based explosive has been developed by McGuire and Tarver [22]:

$$S = -\lambda \nabla^2 T + \rho c_p \frac{dT}{dt} \tag{1}$$

where, S is the chemical heat source during the chemical reaction, λ is the thermal conductivity, ρ is the density and c_p is the specific heat. The scheme proposed by McGuire and Tarver's model reaction for RDX based explosives is a 3 step kinetic model where mass is converted from one species to another:

$$A \overset{k_1}{\rightarrow} B \overset{k_2}{\rightarrow} 2C \overset{k_3}{\rightarrow} D \quad (2)$$

In which A=RDX, B=H_2C, C=CH_2O+N_2O and D=final gaseous products. Each of the reduced chemical reactions follows the Arrhenius equation:

$$k = AZe^{(-E/RT)} \quad (3)$$

Where k is the reaction rate coefficient, Z is the frequency factor (collision number), E is the activation energy and A is the molar fraction. In our model the full reaction is modeled as an instantaneous one step exothermic chemical reaction thus, A is taken to be 1 and heat generation is calculated with the equation (4).

$$S = \rho Q_{act} A Z e^{(-E/RT)} \quad (4)$$

Temperature dependent heat generation term (1) using constants for PBXN-109 given in Table 1 is implemented into Fluent with a user defined function (UDF), [27].

Table 1. Heat Generation Constants, [27]

ρ [kg/m^3]	Q_{act} [J/kg]	Z [1/s]	E [J/mol]	R [J/mol.K]
1680	2198070	1.023x10^{14}	152716	8.314

After defining the kinetic model for the thermal decomposition of the explosive, it is necessary to define the boundary condition to be able to solve thermal conduction heat transfer to explosive. There is a boundary condition definition proposed by Victor [13] where temperature is assumed to be constant throughout the test and is 1073 K with a convection coefficient of 6 W/m^{2}K and emissivity of 1. Applying heat flux as a boundary condition is another option. There are some studies going on by Fuel Fire Experts (FFE) Working Group [28] to measure heat flux rates and compare the data with the alternative fast cook-off test measurements. This is being done to check if there is any alternative method eligible to mimic standard hydrocarbon fuel

fire thermal load. Measurements within the hearth of fire shows that, heat flux values vary between 100-150 kW/m^2 [29].

The most time consuming but accurate way of predicting the time to reaction is probably modeling the fire itself instead of applying the thermal load as a boundary condition. There are some examples of fire modelling codes such as C-SAFE [30] Sierra/Fuego [31] and LES solvers [32]. But as these codes are not available for commercial use and requires huge amount of computational work, it has been decided to go on with the effort of finding the least time consuming and "accurate enough way" of predicting the time to reaction.

Although 1-D (infinitely long cylinder approach, axisymmetric) thermal analysis approach might satisfy the current geometry of our generic test item, most of the time because of the complex geometrical shapes of the energetic systems this is considered not to be applicable. Thus, only 2-D and 3-D thermal analysis are performed, using commercial ANSYS Fluent software as it is commonly used in similar applications [33], [34]. The aim is to conclude to a point of an improved boundary condition definition and to see how accurate the predictions are from the analysis.

Both 2-D axisymmetric and 3-D transient analyses are performed with pressure based solver as it is known to be better performing for incompressible low velocity flows [35]. 3-D analyses are made in order to see the effect of buoyancy (trapped heated air within the test chamber).

Gravitation force is enabled in order to let heated air move within test chamber. PISO (Pressure-implicit with splitting of operators) pressure-velocity scheme is used because of the limitations of the SIMPLE and SIMPLEC is that new velocities and corresponding fluxes do not satisfy the momentum balance after the pressure correction equation is solved. Although the PISO algorithm takes more CPU time per solver iteration, it can dramatically decrease the number of iterations required for convergence, especially for transient problems [35].

For spatial discretization, second order for energy and momentum whereas body force weighted discretization is chosen.

For 2-D analysis, constant density is defined for the air inside the test chamber, the convection and radiation terms are applied as boundary condition; leaving the energy equation with the heat generation and conduction term only.

2.2. Post-Ignition Phase: Ventilation of Explosive Burn Products

To be able to determine the critical ventilation area, the mathematical model of the system shall be derived first. Reaction of PBXN-109 like any other energetic material that contains its own oxidizer produces burn products that fills and pressurize the free volume of the container. Ventilation on the other hand will discharge burn products that will produced by the burn of energetic material. To solve this problem free volume within the chamber is defined as the control volume having one inlet and one outlet as shown in Figure 8. Inlet in this case represents the total burn area whereas outlet represents the total area of ventilation precautions.

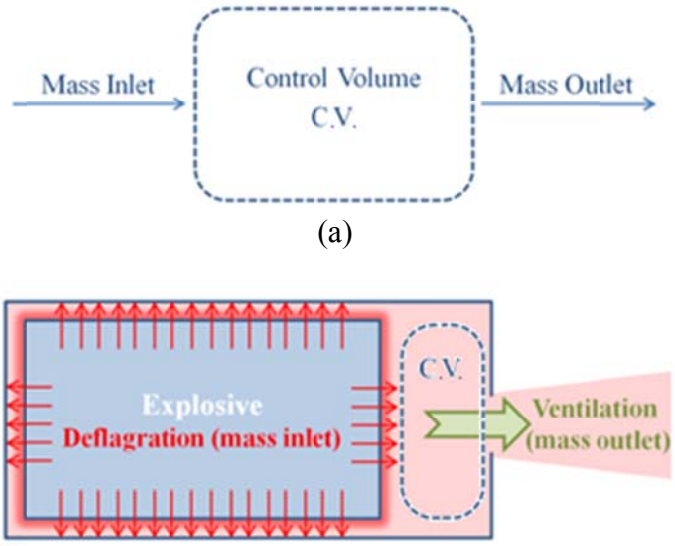

Figure 8 (a) Schematic of the Problem Description of Critical Ventilation Problem, (b) Detailed Description of the Mass Inlet and Mass Outlet

As the purpose of this work is to predict critical ventilation area, it is possible to assume that the flow is choked and Mach is equal to one at the orifice ventilation hole. The aim here is to assume that the ventilation at its highest rate and see if the pressure within the chamber is still rising or not. As long as the initial pressure that is described in the problem tends to decrease this will point out that the ventilation diameter will not cause a dangerous situation where the burn speed of the explosive diverge, cause it to deflagrate and even explode with the pressure increase. So, one can basically write conservation of mass equations to solve this problem assuming that the burn area of the explosive is constant (no burn back).

As shown in Figure 8, problem can be defined with a single mass inlet (explosive burn products) and a single mass outlet (total ventilation area). As long as explosive self-ignites due to heat generation, burn products will start to fill chamber increasing the pressure within and exiting the chamber due to pressure difference with respect free atmosphere.

$$\dot{m}_{inlet} + \dot{m}_{outlet} = \frac{d(m_{build\ up})}{dt} \tag{5}$$

The rate of mass transfer to the control volume can be defined as the product of total explosive area A_{burn}, burn speed of the explosive r_{burn} and the density of burn products within the chamber ρ_{burn}.

$$\dot{m}_{inlet} = A_{burn}.r_{burn}.\rho_{burn} \tag{6}$$

As the chamber pressure exceeds the outside pressure (atmospheric pressure) by a ratio more than 0.8 MPa, the flow becomes sonic for air [26]. Thus, mass transfer from the control volume can be solved at the section where Mach number is assumed to be 1 and very simple expression for the rate of mass discharged results in equation 7. Although this ratio will change for burn products the same approach can be

$$\dot{m}_{outlet} = A_{vent}.u^*.\rho^*.C_D \tag{7}$$

where C_D is the discharge coefficient. It is generally used as 1 in ideal flow but in actuality, because of the ventilation hole shapes (square-edged orifice) that results in a coefficient of 0.82 is used as vena contracta is formed by the exiting gases [36].

Unknown terms at the orifice can be solved using the isentropic equations given below (8, 9, 10, and 11) [36].

$$\rho^* = \frac{P_{vent}}{RT_{vent}} \tag{8}$$

$$u^* = \sqrt{\mathrm{k}RT_{vent}}M \tag{9}$$

$$P^* = \frac{P_{chamber}}{\left[1 + \frac{k-1}{2}M^2\right]^{\frac{k}{k-1}}} \tag{10}$$

$$T^* = \frac{T_{chamber}}{\left[1 + \frac{k-1}{2}M^2\right]^{\frac{k}{k-1}}} \tag{11}$$

Burned explosive gaseous product properties in the chamber of the test item are obtained from the NASA Chemical Equilibrium and Applications (CEA) software [37] by modelling the PBXN-109 components as given in Table 2.

Table 2. PBXN-109 Gaseous Product Thermodynamic Properties in Chamber from NASA CEA Software

Input			
	Reactant	**Weight Fraction**	**Energy [J/Mol]**
1	Al	0.21	0.00
2	HTPB	0.08	-260.17
3	IPDI	0.01	-372249.00
4	DOA	0.07	0.29
5	RDX	0.63	66984.78
6	Antioxidant	0.00	-165587.00
Output			
Burn Product	**Temperature [K]**	**Cp [J/g.K]**	**λ**
	2552.94	1.92	1.22

Although definition of constant burn area is enough for defining the critical ventilation area, it is also possible to define burn area as a variable with respect to burn rate (∀) of the energetic material as shown in equations (13) and (14).

$$\forall = \forall_{initial} + \int (A_{burn} . r_{burn}) dt \tag{13}$$

$$r_{burn} = a . P_{chamber}^{n} \tag{14}$$

a and n should be known in order to solve this problem. Like other HMX (octahydrotetranitrotetrazine) and RDX energetic materials, PBXN-109 also has burning characteristics that is affected by the change of pressure and temperature [38]. There are some studies in the literature for characterizing the burning rate of both pure RDX [39] and PBXN-109 [40]; however they are mostly made over pressure values of 10 MPa. Although there are some applications where warheads can withstand to very high internal pressures (hard target penetrators), most of the time warheads are not designed to withstand internal pressures of those values mentioned above. To be able to model low pressure burning of the explosive and calculate critical ventilation area, strand burner tests are conducted with the prepared samples of PBXN-109. Above given equations are implemented into a MATLAB Simulink body as shown in Figure 9. MATLAB Simulink tool is preferred because of it's easy to use interface and graphical output capabilities.

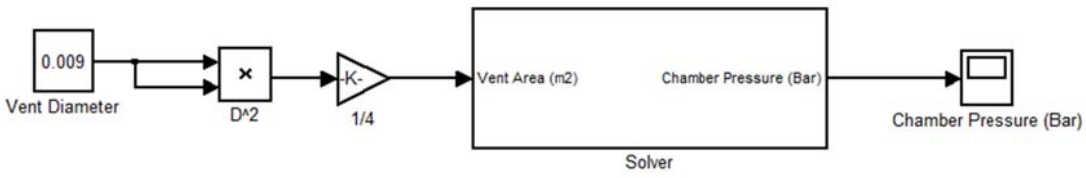

Figure 9. MATLAB Simulink –Main Body

Main body basically uses the "input.m" file for initials and variables such as burn rate coefficients and explosive thermodynamic constants. This file is given in Appendix A. Solver that is used in main body is given in Figure 10 where as two functions of the solver which are Explosive Geometry and Burn Rate is given in Appendix A.

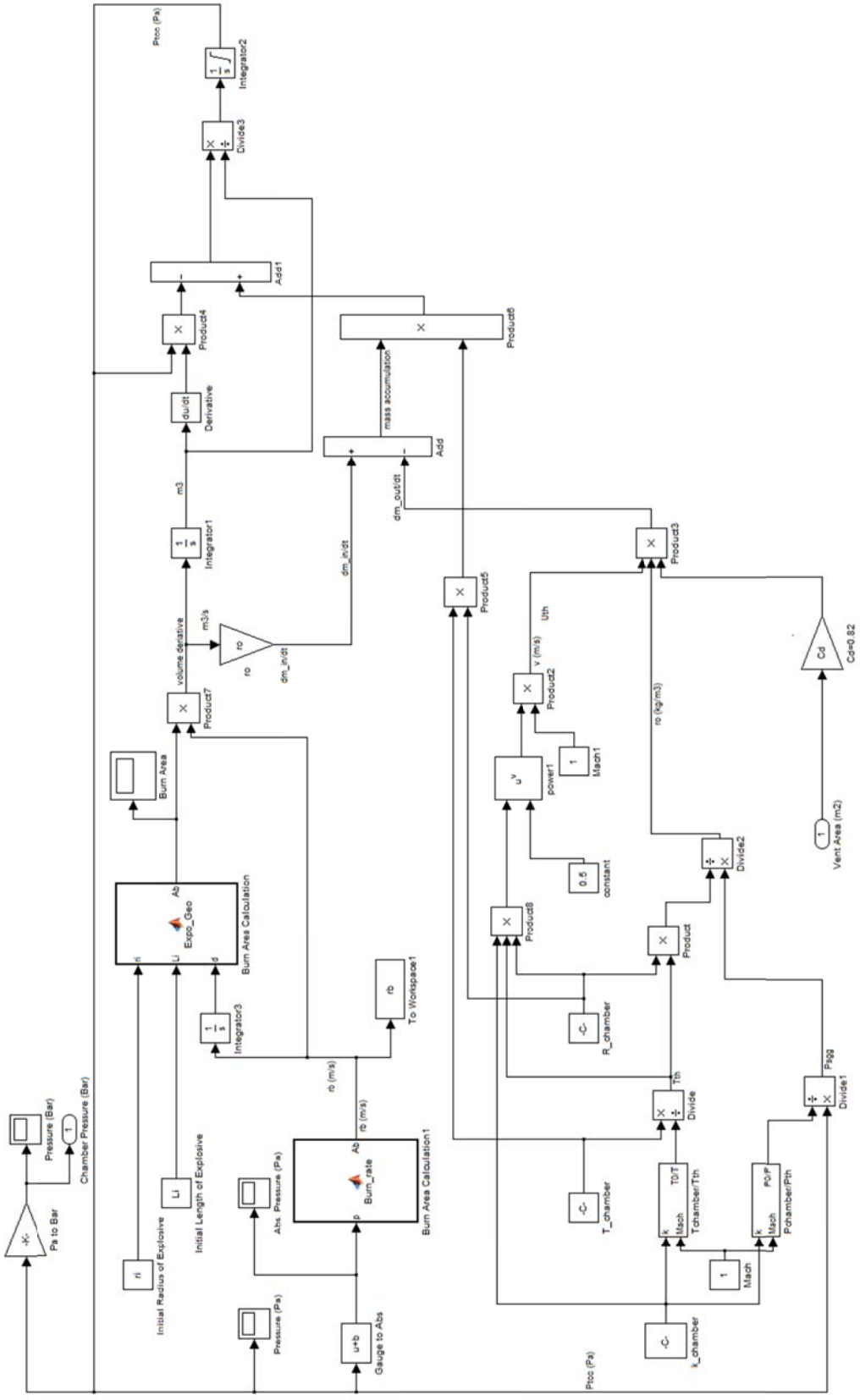

Figure 10. MATLAB Simulink – Solver

CHAPTER 3

CHARACTERIZATION OF THE PBXN-109 EXPLOSIVE

3.1. STRAND BURNER TESTS

Similar to its previous applications [41], strand burner test setup of TÜBİTAK SAGE shown in Figure 11 is used to measure pressure dependent burn rate of the energetic material.

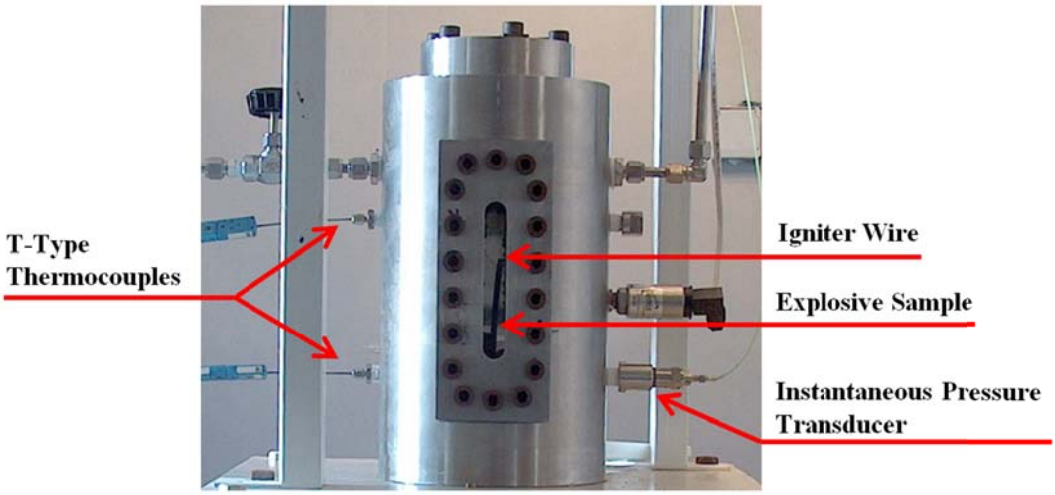

Figure 11. Strand Burner Cylindrical Vessel

Explosive samples are ignited by igniter wires and burned inside the high-pressure strand burner vessel in a continuous pressurized nitrogen supplied environment under well-controlled operating conditions. Figure 12 shows schematic view of the experimental setup.

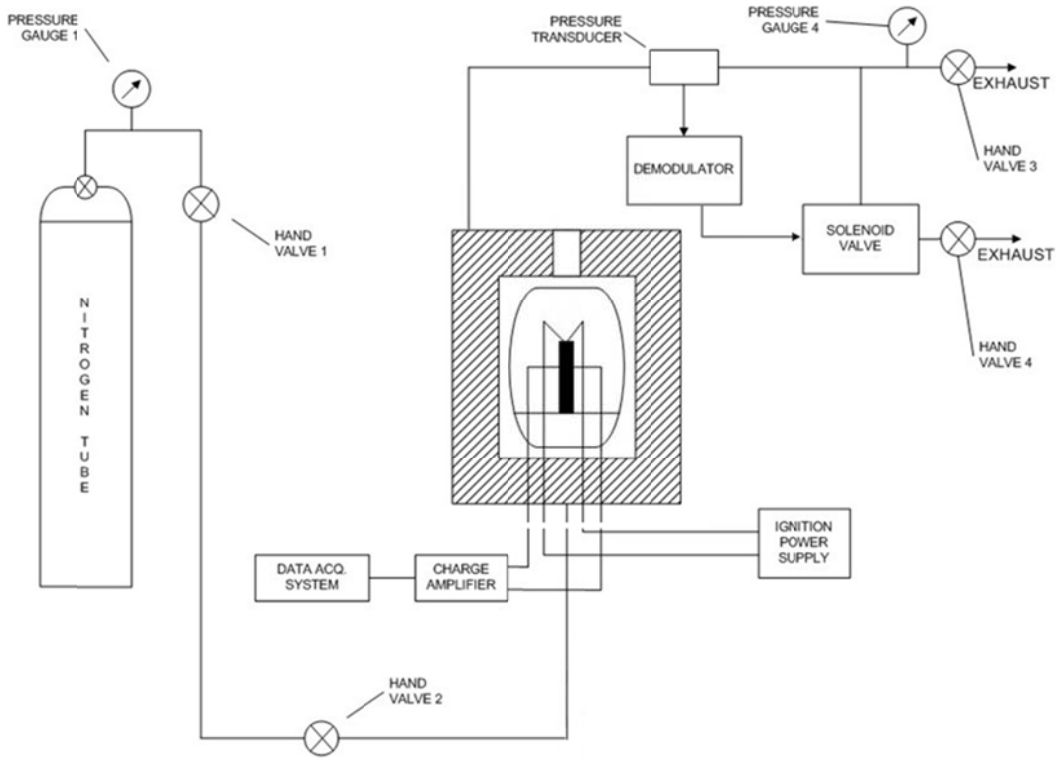

Figure 12. Schematic of the Strand Burner Experimental Setup

Single piece of nichrome wire is used to ignite explosive samples. An electric current is applied through the nichrome wire by an external power supply and ignition occurred as the wire heated. Approximate resistance of the nichrome wires are 3 ohms while the external voltage that is used to start ignition is 24 Volts.

The strand burner is pressurized to the desired pressure by high pressure nitrogen gas with a manual operated needle valve. Nitrogen which is an inert gas is especially selected for the tests, by this explosive combustion is not affected with the environmental conditions.

KISTLER pressure transducer (model RAG25A200BV1K) is used to measure static pressure within the chamber. Pressure inside the vessel tends to increase during the explosive burning as the gas generation takes place from the burn front. Pressure stability in the vessel during the test is maintained by a pressure control system, which includes a computer controlled solenoid valve. This valve is used for the discharge of burn products after the explosive ignition.

In our tests, 3 make wires are used to measure burn rate of the explosive. Four holes are drilled on the explosive samples. The first hole is used for the placement of igniter wire where it is located on the near top end of the sample. The other three holes are equally spaced between each other with 30 mm of displacement and used for the placement of make wires (Figure 13).

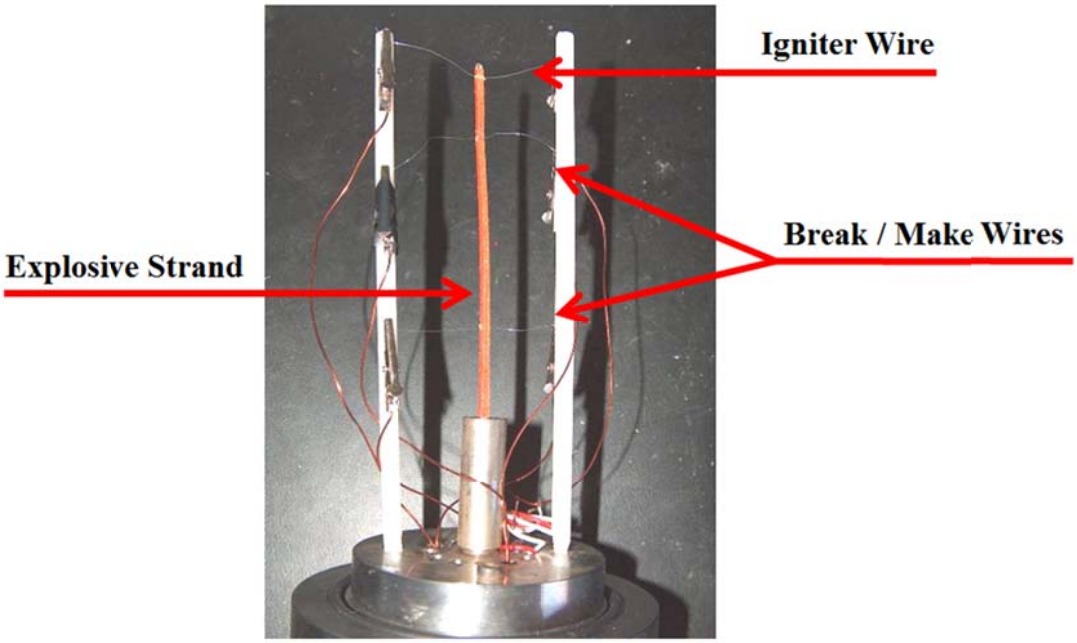

Figure 13. Sample Holder and Wire Connections

Generally, break wires are preferred for the burn rate measurements of propellants at TUBITAK SAGE. But in our applications, we have experienced that the use of break wires can cause problems as sometimes these wires are not breaking or breaking with a delay after burn front passes the location of the wire etc. Break switches are connected to a circuit and are monitored if the supply voltage is valid during the test. During the pass of burn front from the location of break wire they tend to break so that the monitored voltage is no more 5V but instead 0V. Unlike break wires, make wires do not used for monitoring continuous supply voltage. Make wires are simply two isolated cables that are wrapping on each other. As they are isolated they do not let electric to pass one to another. But as the isolation starts to burn connectivity between two wires increases or are just short cut. Due to the monitoring problems with break wires process has been reversed and instead of monitoring the cut signal,

short signal is monitored. A sample, monitored data from a test (PBXN-109, 2 MPa) is shown in Figure 14. Although all three signals have noisy oscillation between ± 1V contact signal can be observed clearly.

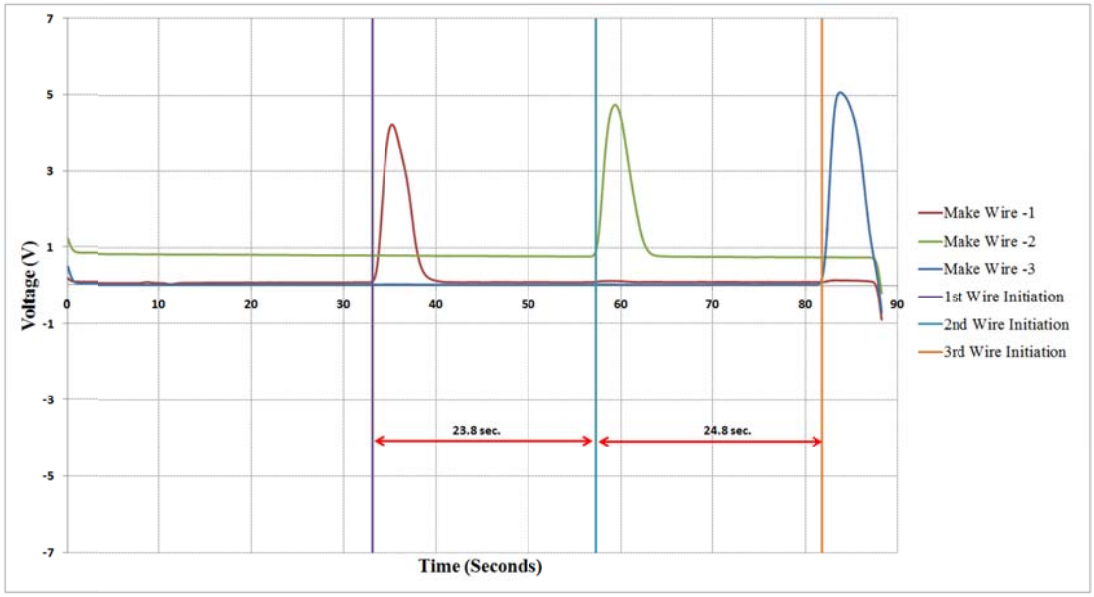

Figure 14. Sample Make Wire Readings

Five different pressure ranges is tested between 2-10 MPa with three repetitions. Unfortunately, below 2 MPa range, it is observed that the explosive cannot sustain the flame front and tend to burn out just after explosive is ignited. Measured burn rates of PBXN-109 are given in Figure 15 and Figure 16 with some literature data. Although there seems to be a discontinuity between the curve fit data of 1-10 MPa and 10-500 MPa, test data made by the Livermore for 10-20 MPa is consistent with the data obtained within this study.

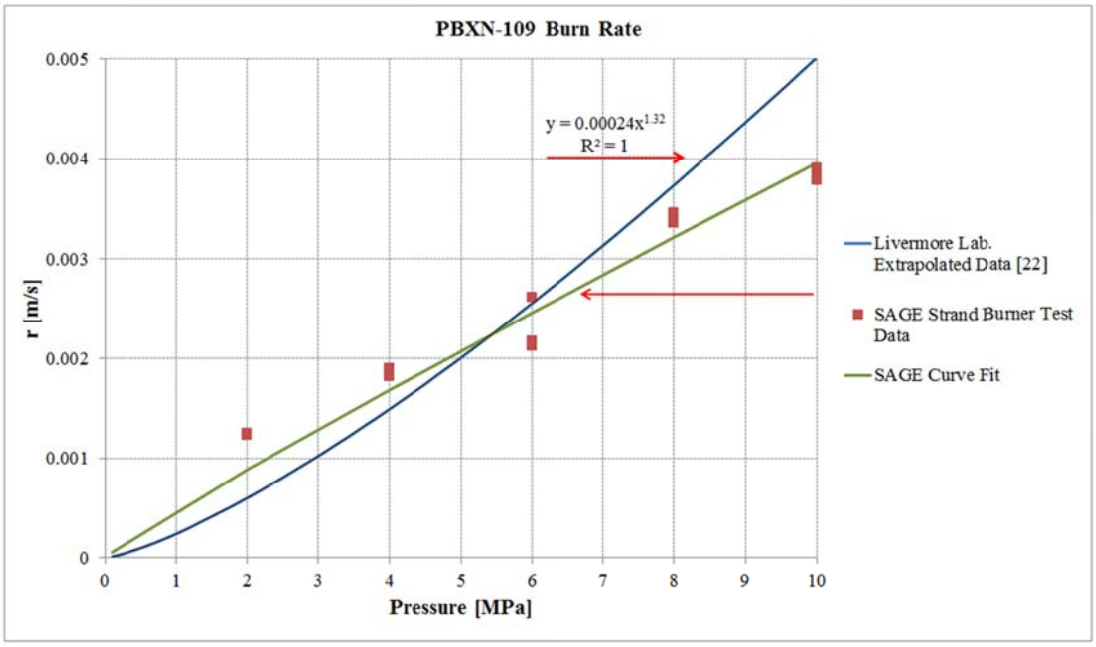

Figure 15. PBXN-109 Burn Rate Change with Pressure (0-10MPa)

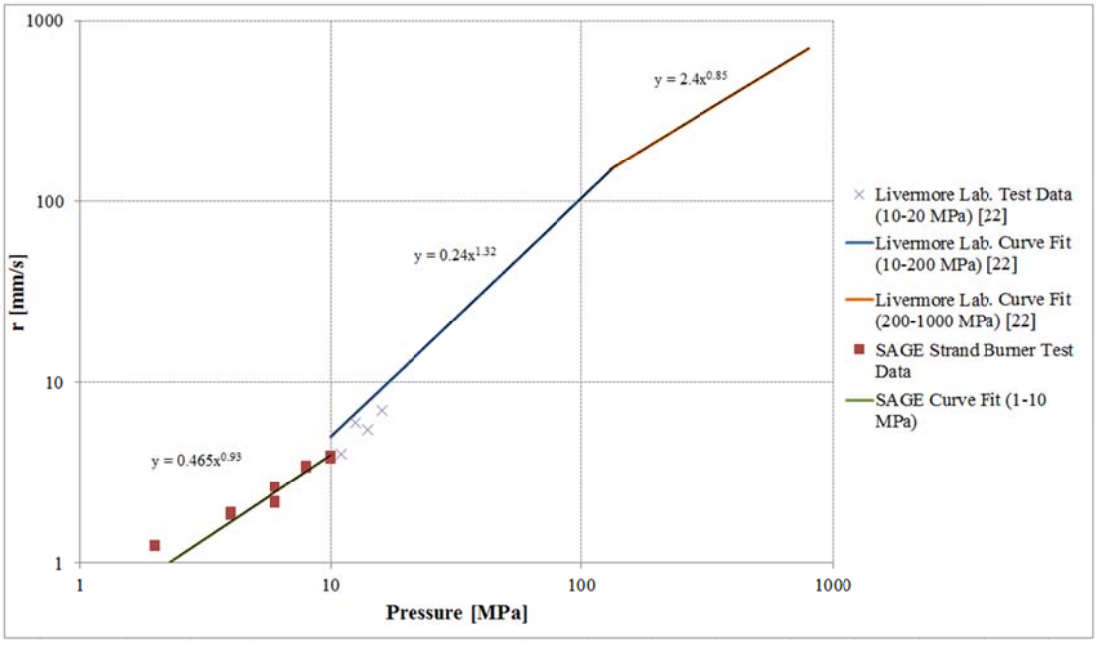

Figure 16. PBXN-109 Burn Rate Change with Pressure (1-1000MPa)

CHAPTER 4

FAST COOK-OFF TESTS

4.1. Description of the Test Item

There are 2 different types of test items which differ on the length of explosive contacting cylinder casing. The length ratio over test specimens are about ¾ and designed to investigate if there is an effect of length on time to reaction. The short test item is shown in Figure 17. Two different liner types (HTPB based thermoset liner and a thermoplastic liner) and two different thicknesses (1 mm and 3.5 mm) are tested. Ventilation holes are closed by an eutectic material developed by TÜBİTAK SAGE that can melt at temperatures around 400 K. Thickness of the plugs are tested and chosen to be thick enough so that they will not melt completely and let flame enter the test chamber before the ignition starts. Plugs are manufactured after each test as thread or tight fit according to the ventilation diameter choice.

Test items are designed so that one can be able to take internal measurements such as temperature and burning rate from the internal parts as shown in Figure 17.

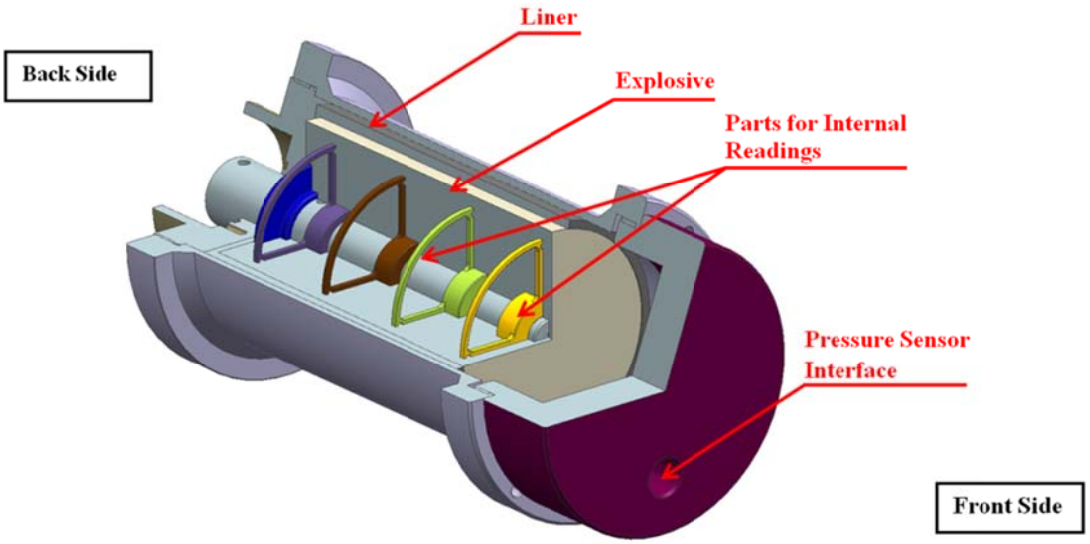

Figure 17. Generic Test Item (Short Version)

There are 4 steel sections located on a polycarbonate rode within the test item and there are 4 inner and 4 outer holes in every section located at 90 degrees to each other. Make switches are connected to these holes in order to locate how the burn front is moving within the explosive during the test. The rod is designed as there is a hole that let make switches come through the back plate of the test item. The rod and the sections are assembled to the test item before the explosive is cast. The hole on rod that cables of make switches are passing is filled with a silicone before the casting. Silicone is also used for preventing short circuit between make switches. The application is shown in Figure 18.

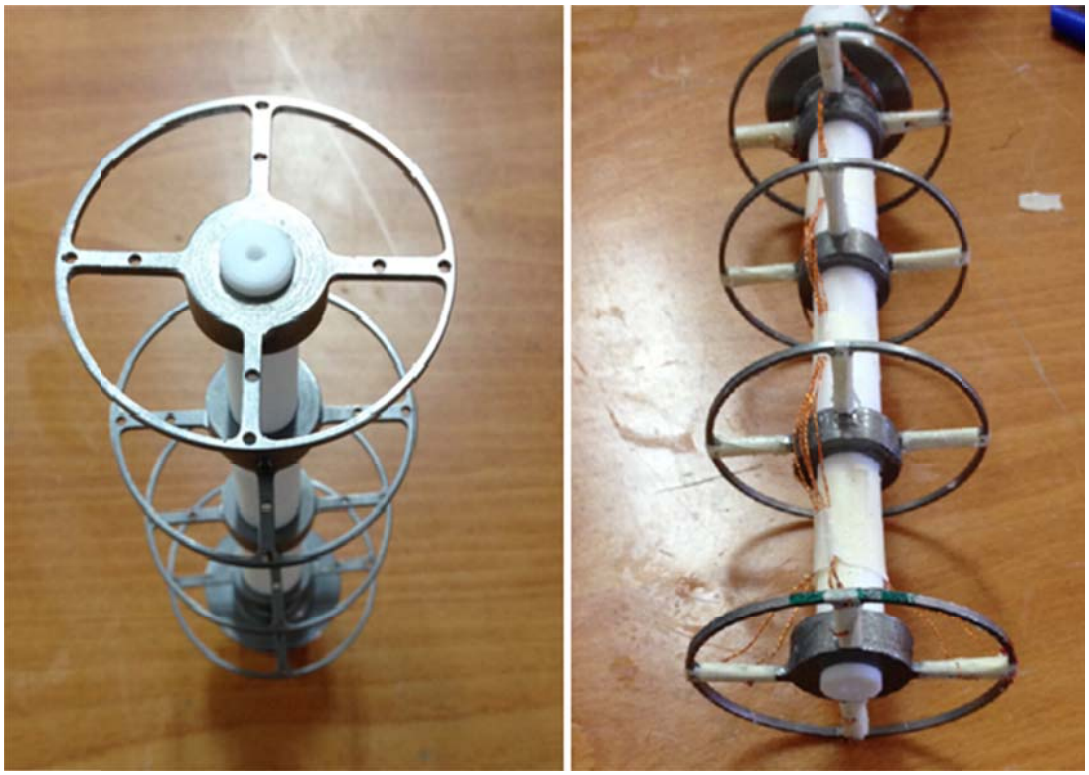

Figure 18. Polycarbonate Rod for Holding Steel Sections Together Within the Explosive

Some pre-analysis is made to ensure that the application of internal reading parts added to test item do not affect the heating rate over explosive and hence do not change time to reaction. However, insulation at the back of the test item should be applied in order to protect the cables out of the test item. Although insulation at the

back side does affect the heating regime over the test item, ignition point of the explosive does not change.

Other than internal readings, one pressure sensor (KISTLER RAG25A80BV1K) and one temperature sensor (ORDEL KTTE3x0.50 5K) are used on the test item. As flame temperatures are expected to be around 2500 K according to the NASA CEA solutions, thermocouple has been placed close to wall to avoid bead getting into ventilation flow path of burn products of explosive and becoming too hot and destroyed. To protect the pressure sensor from the high temperature environment it is placed (buried) outside of the test pool. Connection of the sensor to the test item is made via Ø3 mm stainless steel pipe. The volume increase of test chamber by adding a pipe for the connection of the pressure will delay the instantaneous pressure readings due to additional volume added.

4.2. Experimental Setup

Tests have been performed with the mini fuel fire test setup as the test item dimensions are within the range of declaration of NATO standard 4240 [41].

Total of eight surface thermocouples (STC) is used to measure test item surface temperature. Measurements are made both in the front and rear side. Thermocouples are placed circumferentially with an angle of 90º (Figure 19). To avoid contact dislocations and increase the heat transfer to STCs a thermal paste (Thermigrease TG 20033) is used which can withstand temperatures up to 1200°C and has relatively high thermal conductivity.

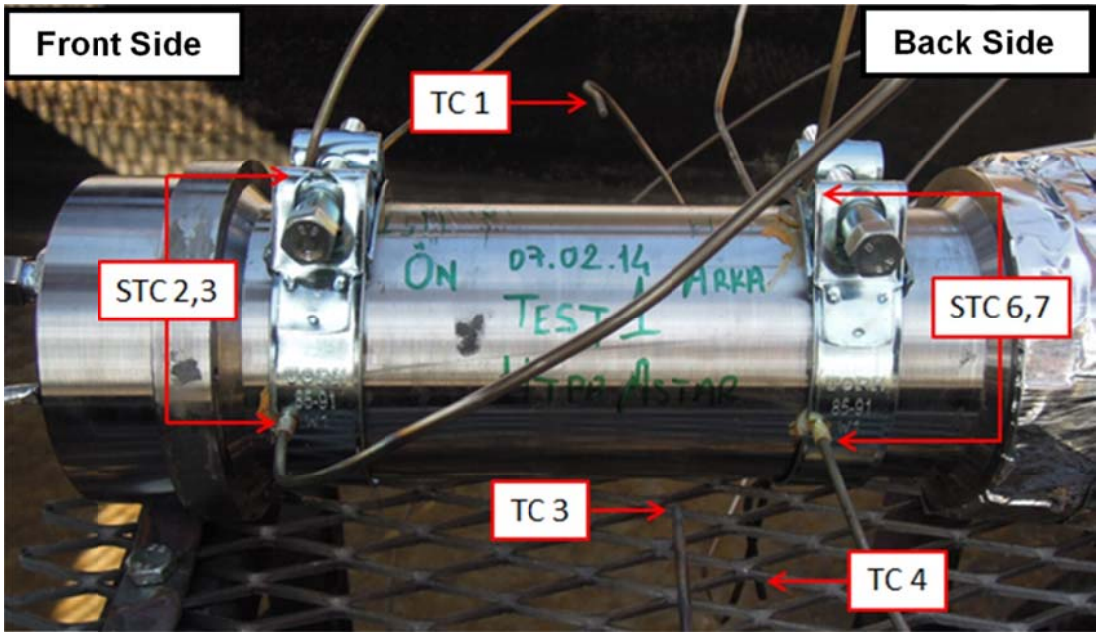

Figure 19. Thermocouple Placement on 1st Test Item

Total number of 8 tests has been made for the determination of TtR and critical vent area. Although there are no internal measurements taken from inside of test case in some tests, back side of those test items are still isolated to simulate the same conditions with previous tests.

Temperatures measurements are taken with 100 Hz whereas pressure and make switch measurements are taken with 1000 Hz by our data acquisition system. (Mrel Data Trap 2 – S/N: 9077)

CHAPTER 5

RESULTS AND DISCUSSION

5.1. Fast Cook-Off Test Results

5.1.1. Test 1

Test item 1 is a long version of two types. It has a ventilation hole diameter of 32.9 mm. It has a 3.5 mm of HTPB liner between the explosive and the casing. As mentioned above the difference of test 1 and other test items is that there are surface temperatures on the casing for determination of surface temperature and boundary conditions accordingly. Test item is shown in Figure 20.

Figure 20. Test Item 1 – Before the Test

According to the first inspection made after tests no deformation due to pressure or melting on the test item is observed as shown in Figure 21.

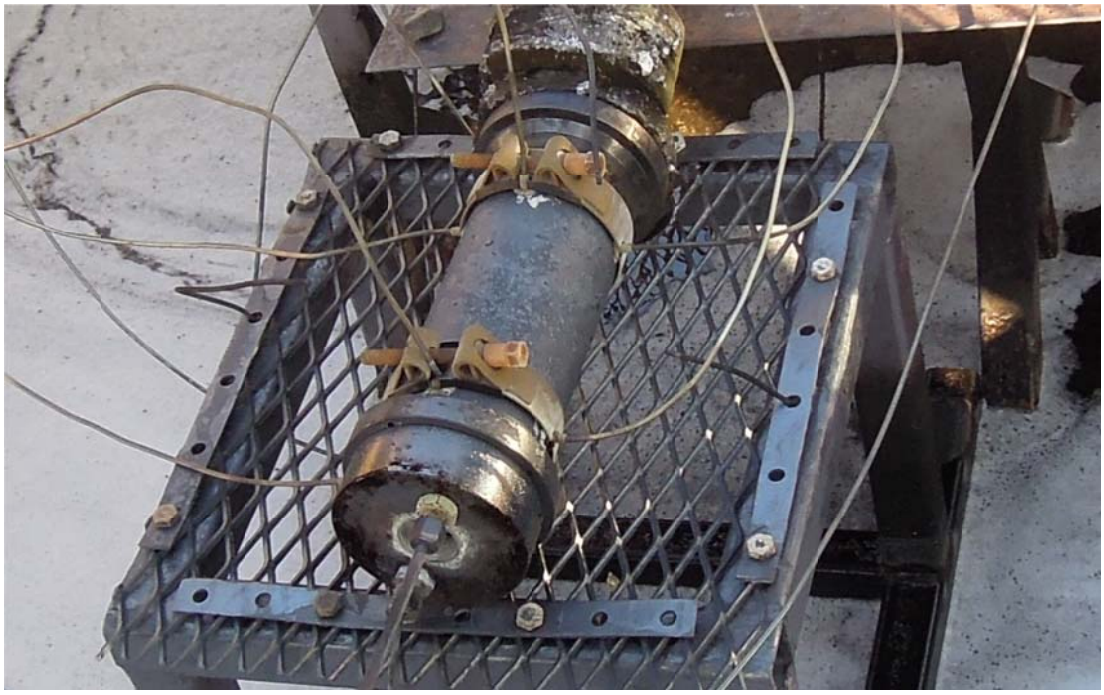

Figure 21. Test Item 1 – After the Test

After the ignition of the fuel within the pool first increase in temperature is detected after 161 seconds of first data is recorded. This is accepted to be the reference time t_0 and other events that are detected during the tests will be referenced to this point.

Temperature measurements are given in Figure 22. Flame temperatures are examined to be appropriate according to the requirements mentioned by the STANAG 4240 [42]. Surface temperatures are taken to evaluation for the determination of boundary conditions and discussed within the comparison of tests with analyses section.

Internal thermocouple readings show that there are two steep increases at t_0+200.4s (361.4s) and t_0+287s (448s). First one is considered to be as a result of the ignition of explosive whereas the second one is due to the hot flame entrance to test chamber after whole explosive burn out.

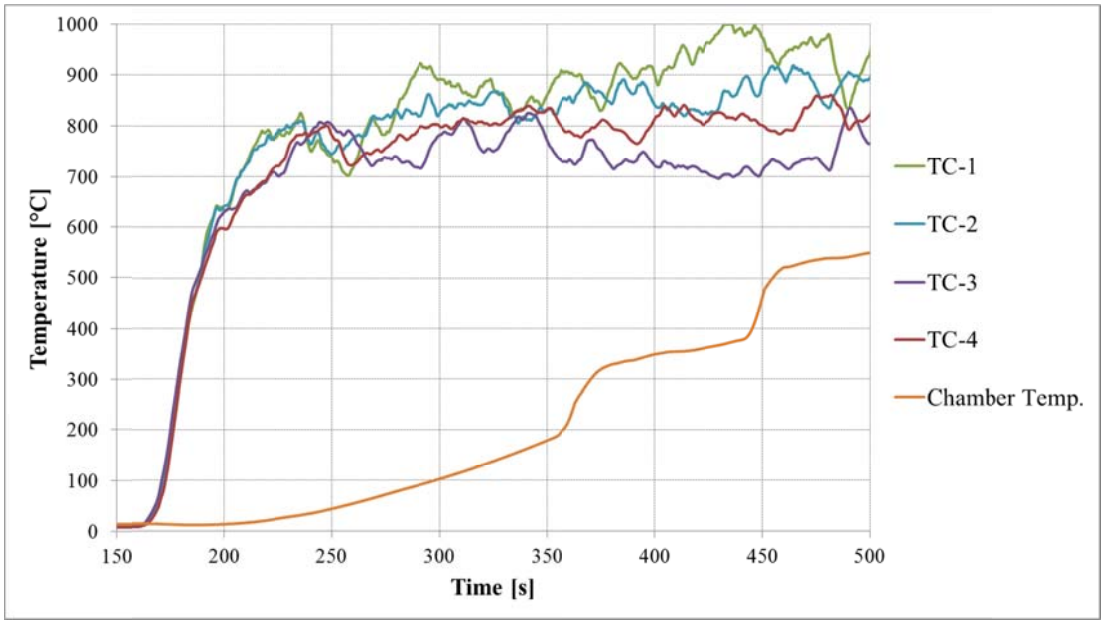

Figure 22. Flame, Surface and Internal Temperature Readings of Test Item 1

Chamber pressure readings given in Figure 23 indicate that pressure within the chamber starts to increase at t_0+200.3s (361.3s) and suddenly drops to "zero" at t_0+213s (374s). Increase of pressure is considered to be the ignition of the explosive whereas sudden drop indicates the removal of ventilation plug debris. As the plug softens (and melts at outer open surfaces to flame) and is estimated that it is no longer eligible to sustain high internal pressures after certain point.

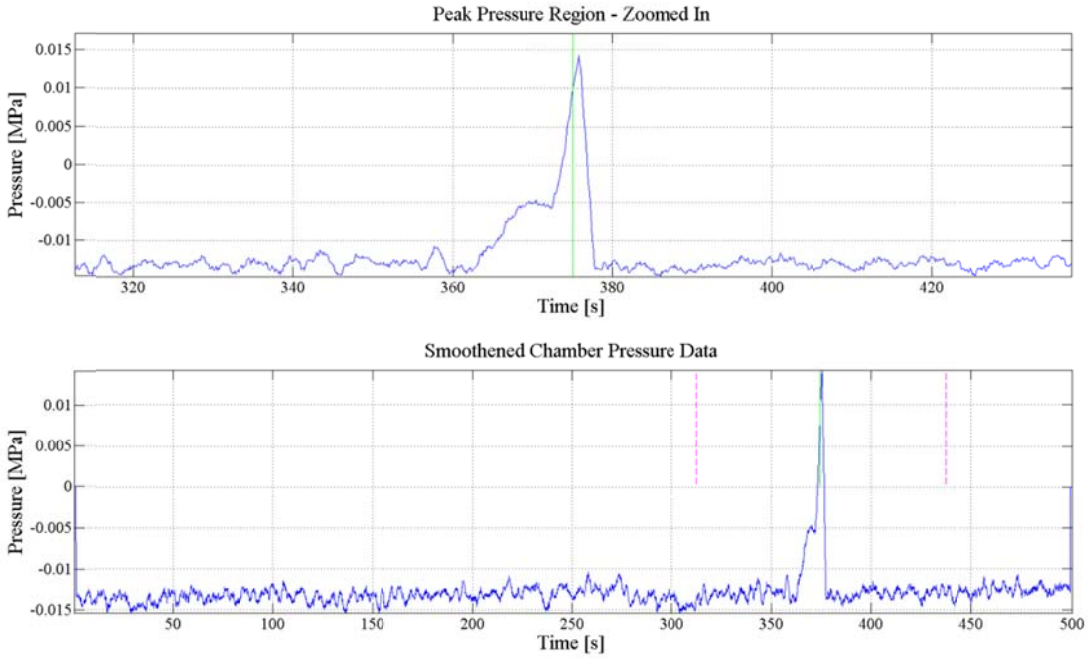

Figure 23. Internal Pressure Readings of Test Item 1

Although cables that are coming out of the test item seems to be well protected, no useful data could be acquired from the make switches that are placed within the test item.

According to the visualization of test video recording and inspection of audio recordings, flame starts to come out of ventilation hole 200 seconds after the first ignition of fuel.

5.1.2. Test 2

Test item 2 is a short version of two types. It has a ventilation hole diameter of 5.3 mm. It has a 3.5 mm of thermoplastic liner between the explosive and the casing. Test item is shown in Figure 24.

Figure 24. Test Item 2 – Before the Test

According to the first inspection made after the test, deformation on the sidewall of the test item due to pressure or melting is observed as shown in Figure 25.

Figure 25. Test Item 2 – After the Test

After the ignition of the fuel within the pool first increase in temperature is detected after 140.2s of first data is recorded. This is accepted to be the reference time t_0 and other events detected during the tests will be referenced to this point.

Temperature measurements are given in Figure 32. Flame temperature readings are observed to be appropriate with STANAG 4240 requirements. Internal thermocouple readings show that there is a steep increase at t_0+171.8s (312s). This is considered to be as a result of the ignition of explosive.

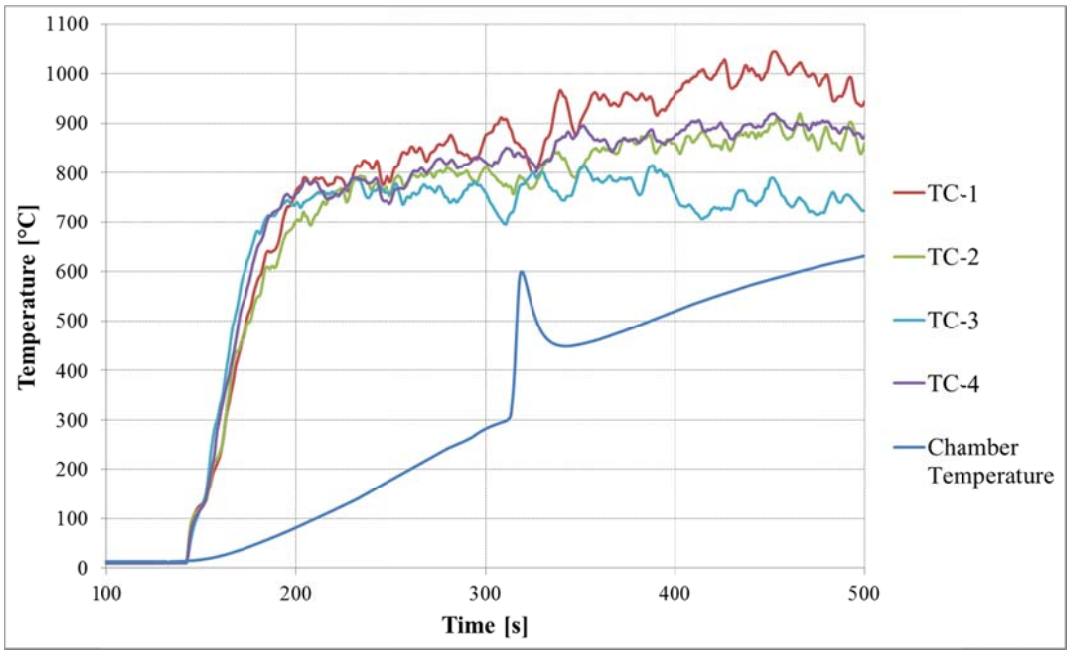

Figure 26. Flame and Internal Temperature Readings of Test Item 2

Chamber pressure readings given in Figure 27 indicate that pressure within the chamber starts to increase at t_0+172s (312.2s) and suddenly drops to "zero" at t_0+178s (318.2s). Increase of pressure is considered to be the ignition of the explosive whereas sudden drop indicates the possible reason of test item side wall being torn.

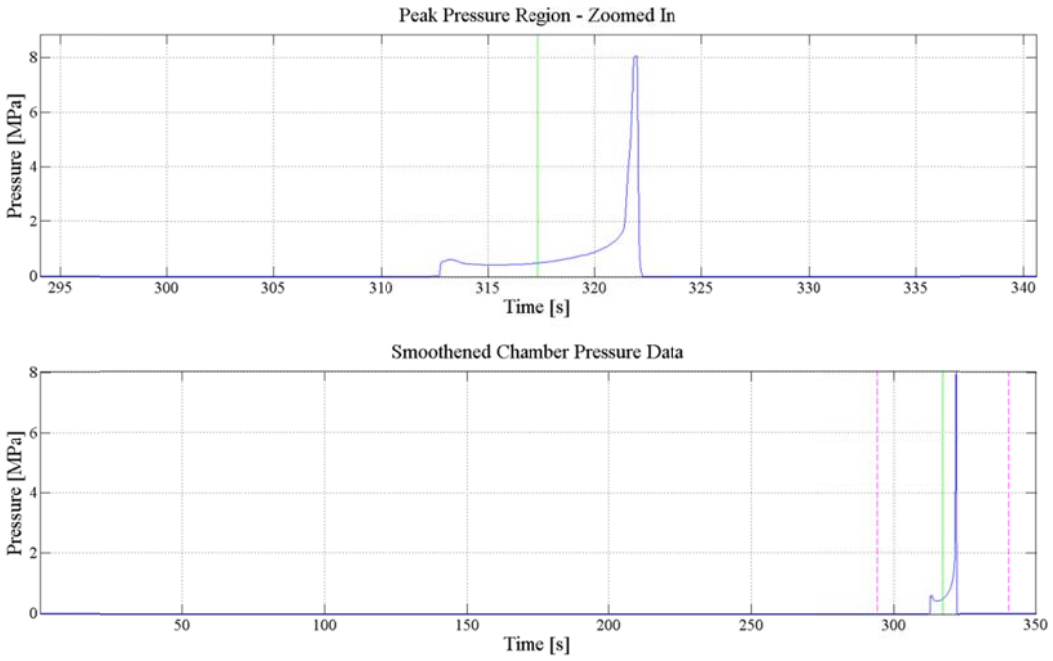

Figure 27. Internal Pressure Readings of Test Item 2

Although cables that are coming out of the test item seems to be well protected, no useful data could be acquired from the make switches that are placed within the test item.

According to the visualization of test video recording and inspection of audio recordings, flame starts to come out of ventilation hole 172 seconds after the first ignition of fuel.

5.1.3. Test 3

Test item 3 is a short version of two types. It has a ventilation hole diameter of 12.3 mm. It has a 3.5 mm of thermoplastic liner between the explosive and the casing. Test item is shown in Figure 28.

Figure 28. Test Item 3 – Before the Test

According to the first inspection made after tests no deformation due to pressure or melting on the test item is observed as shown in Figure 29.

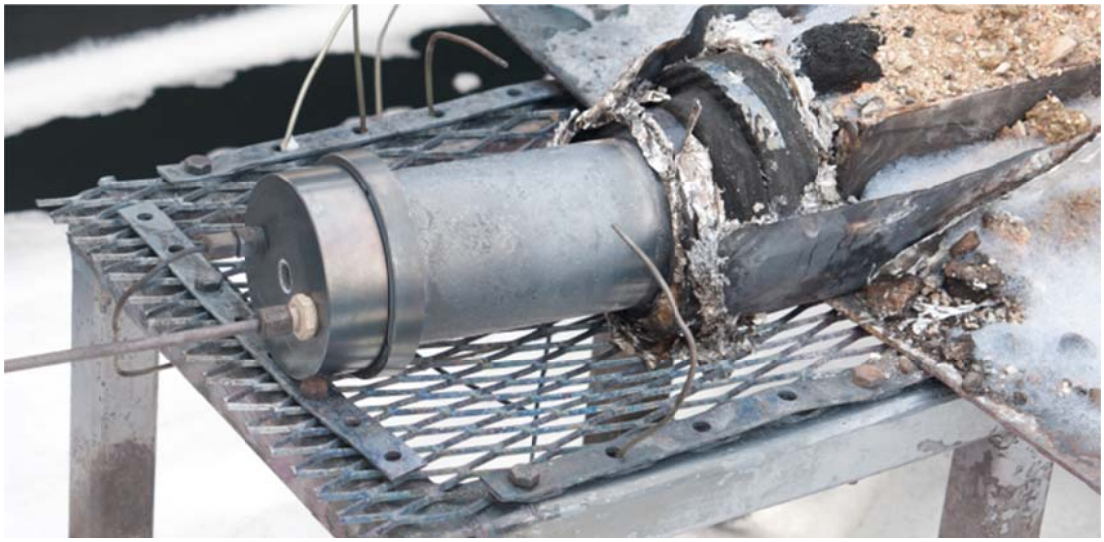

Figure 29. Test Item 3 – After the Test

Instead of using make switches in this application, total of 4 surface type thermocouples are used within the test item. 3 of the thermocouples are placed on the steel section (Figure 30) whereas the 4th one is located on the middle of sidewall (Figure 31) of the test item to measure liner temperature and detect side ignition.

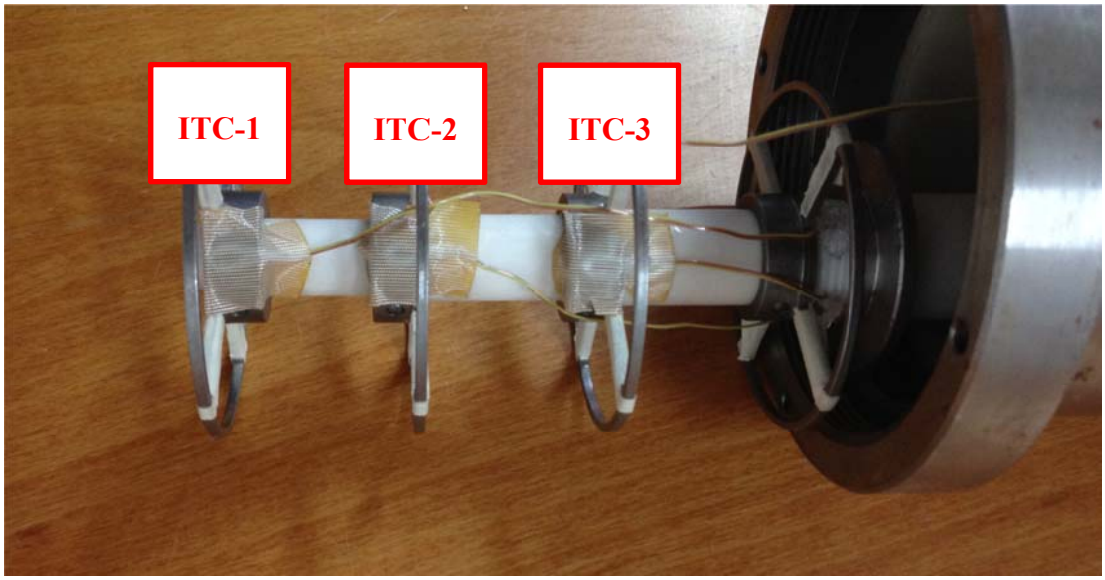

Figure 30. Surface Type Thermocouples That Are Located on the Steel Sections

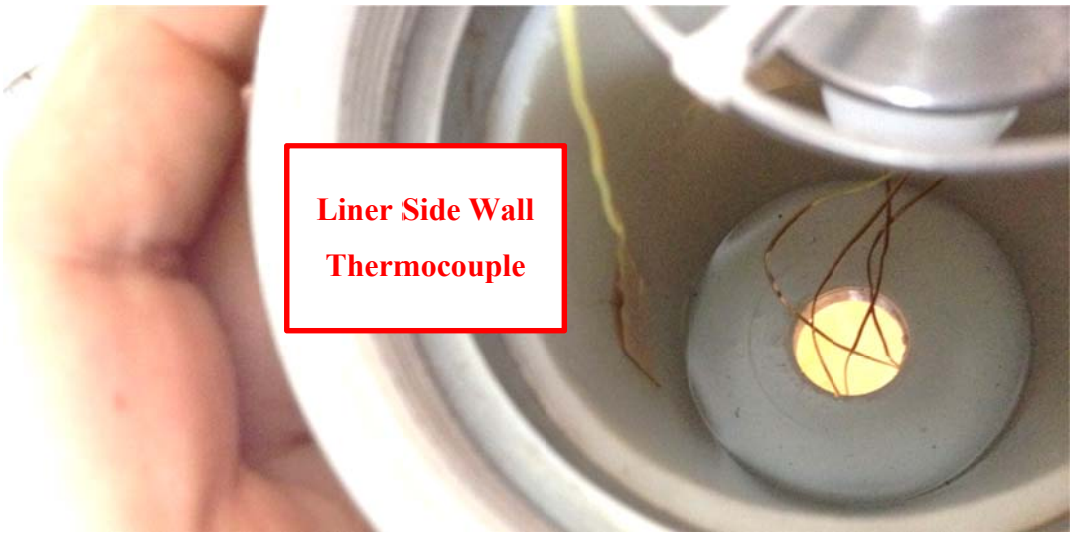

Figure 31. Surface Type Thermocouple That Is Located in the Middle of Test Item Sidewall

After the ignition of the fuel within the pool first increase in temperature is detected after 158 seconds of first data is recorded. This is accepted to be the reference time t_0 and other events detected during the tests will be referenced to this point.

Temperature measurements are given in Figure 32. Flame temperature readings are observed to be appropriate with STANAG 4240 requirements. Internal thermocouple readings show that there is a slight increase at t_0+178s (336s) considering the

temperature increase over the whole test period. This is considered to be as a result of the ignition of explosive. The total increase in temperature during the ignition of energetic materials is less compared to first two tests as the internal thermocouple bead is left within the body of front closure. This is done because to decrease the number of instrumentation failure.

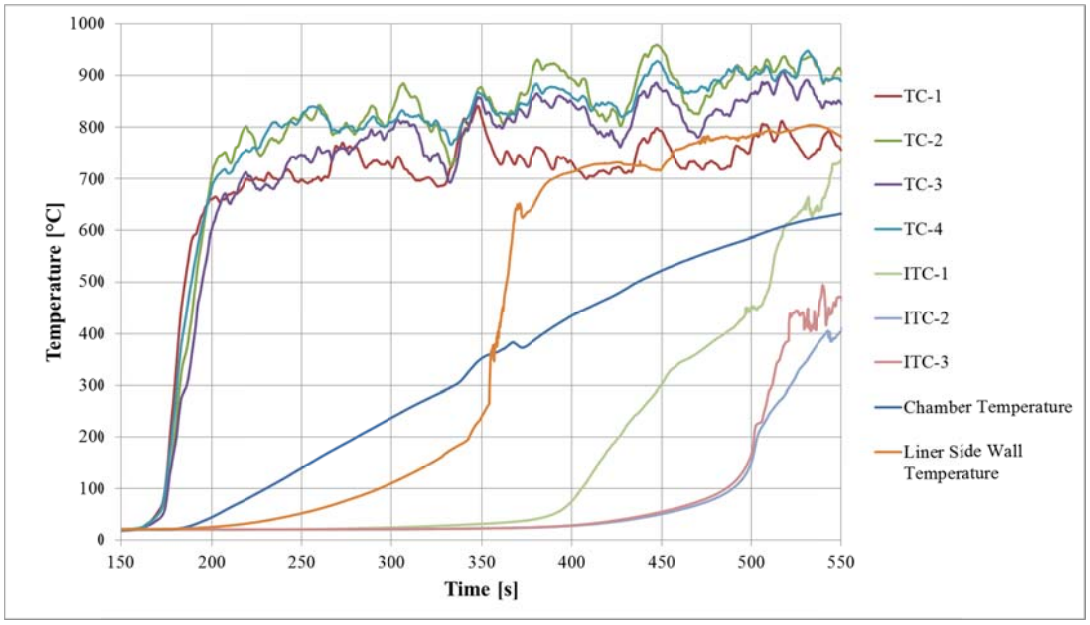

Figure 32. Flame and Internal Temperature Readings of Test Item 3

Side wall temperature starts to increase as the flame within the pool is ignited. At t_0+173s (331s) measured temperature exceeds 200 °C and reaches to critical temperature for PBXN-109. As self-ignitions occur at t_0+178s (336s) a steeper increase in temperature can be observed.

Other thermocouples that are placed on steel sections which are located within the explosive shows slower increase in temperature as the thermal conductivity of the explosive is relatively low. It is observed that these surface type thermocouples were failed to measure flame temperature as the bead of these thermocouples are not protected and break instead. However, the time that flame interacts with the thermocouples are tried to be estimated according to increase rate. It is estimated that burn front surface has interacted with ITC-1 56 seconds after the ignition occurred whereas this time is estimated to be 162 seconds for the TC-2 and TC-3. Relaying on

the assumption that flame covers all explosive surface just after the ignition, explosive burn speed can be calculated by knowing the distance (shortest) of each thermocouple to explosive surface. Using the 3-D model of the test item distances are measured and given in Figure 33. If the calculation is made from the side wall to TC-2 and TC-3 the burn speed of the explosive can be found to be 0.151 mm/s whereas 0.125 mm/s for TC-1.

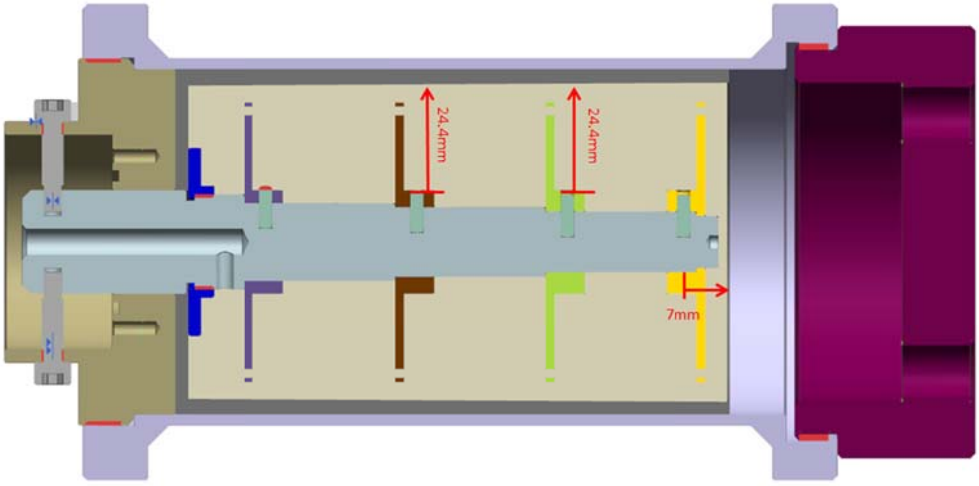

Figure 33. Section View of Test Item 3 and Dimensions from the Measuring Points to Explosive Surface

Chamber pressure readings given in Figure 34 indicate that pressure within the chamber starts to increase at t_0+177s (335s) and suddenly drops at t_0+266s (424s). Increase of pressure is considered to be the ignition of the explosive. The drop at t_0+266s is sudden but the pressure that is measured at that moment is not exactly "zero". This is assumed to be a pressure transducer failure especially with the pressures falling below "zero" after 500 seconds of first data recording.

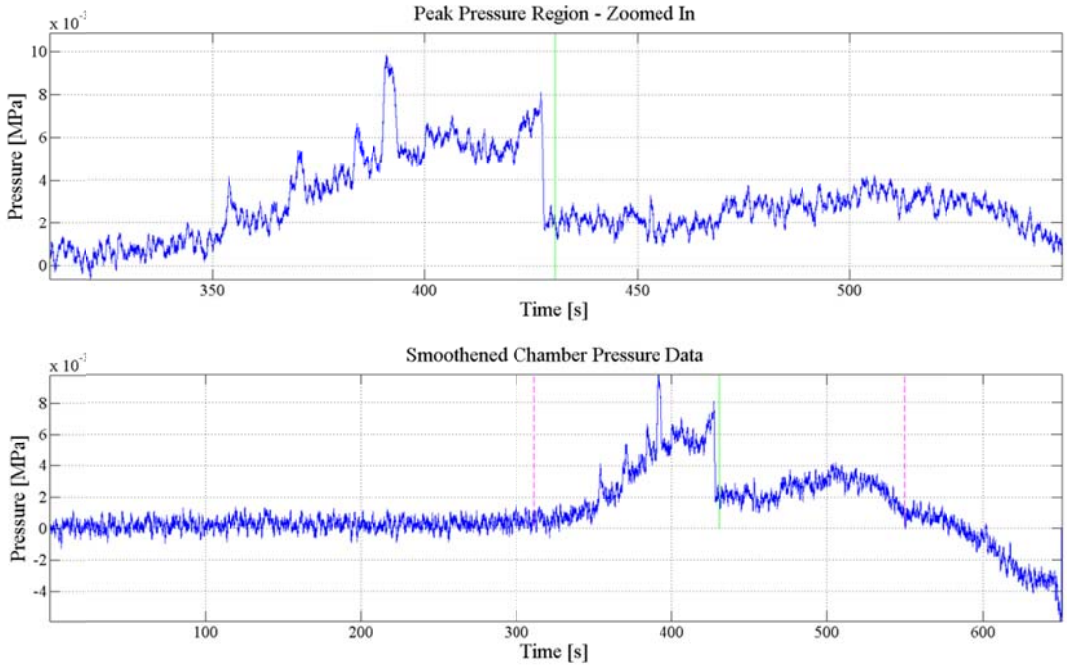

Figure 34. Internal Pressure Readings of Test Item 3

According to the visualization of test video recording and inspection of audio recordings, flame starts to come out of ventilation hole 179 seconds after the first ignition of fuel.

5.1.4. Test 4

Test item 4 is a short version of two types. It has a ventilation hole diameter of 8.7 mm. It has a 1 mm of thermoplastic liner between the explosive and the casing. Test item is shown in Figure 35. There are no make switches are used for this test and further test as no improvement could be made on the application and it has failed to get successful data.

Figure 35. Test Item 4 – Before the Test

According to the first inspection made after tests no deformation due to pressure or melting on the test item is observed as shown in Figure 36.

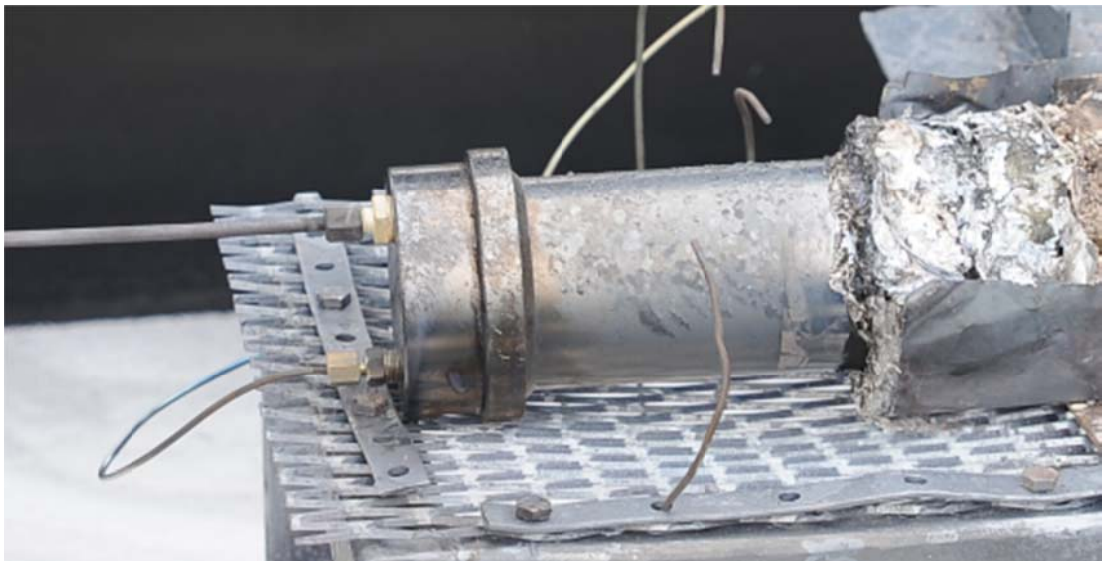

Figure 36. Test Item 4 – After the Test

After the ignition of the fuel within the pool first increase in temperature is detected after 216 seconds of first data is recorded. This is accepted to be the reference time t_0 and other events detected during the tests will be referenced to this point.

Temperature measurements are given in Figure 37. Flame temperature readings are observed to be appropriate with STANAG 4240 requirements. Internal temperature measurements are not given as the thermocouple was failed during the test and no

useful data is obtained. Internal measurement thermocouple is replaced for further tests because lack of thermocouples and it is possible to indicate ignition from the pressure readings.

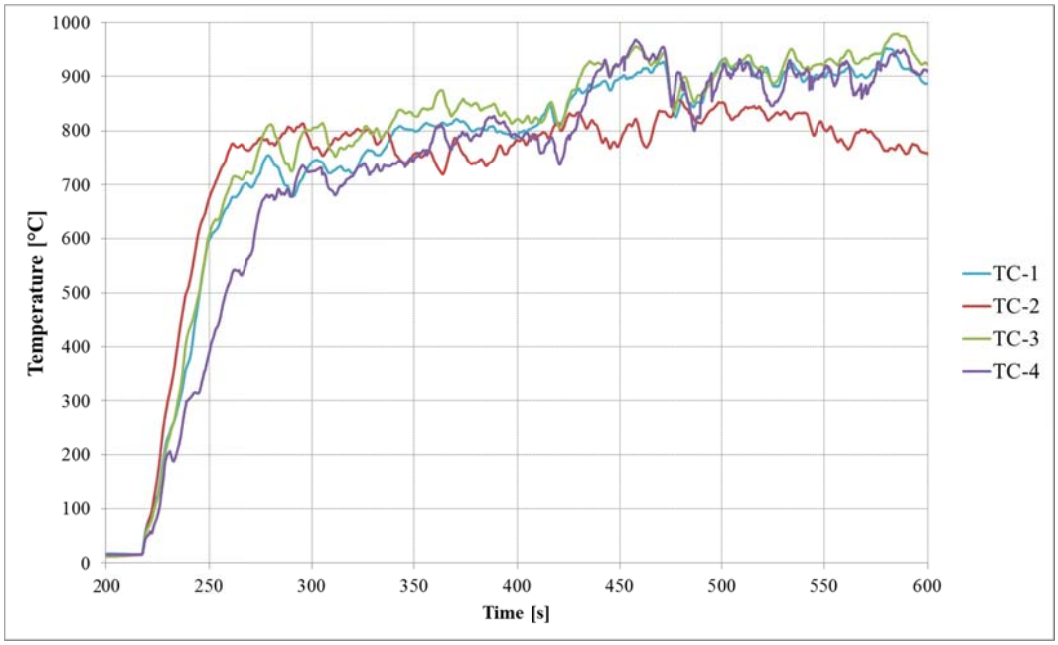

Figure 37. Flame and Internal Temperature Readings of Test Item 4

Chamber pressure readings given in Figure 38 indicate that pressure within the chamber starts to increase at t_0+176s (392s) and suddenly drops to "zero" at t_0+204s. Increase of pressure is considered to be the ignition of the explosive whereas sudden drop indicates the removal of ventilation plug debris. 20 seconds after the pressure drops to zero, it starts to rise to 0.015 MPa and drops to zero again slowly.

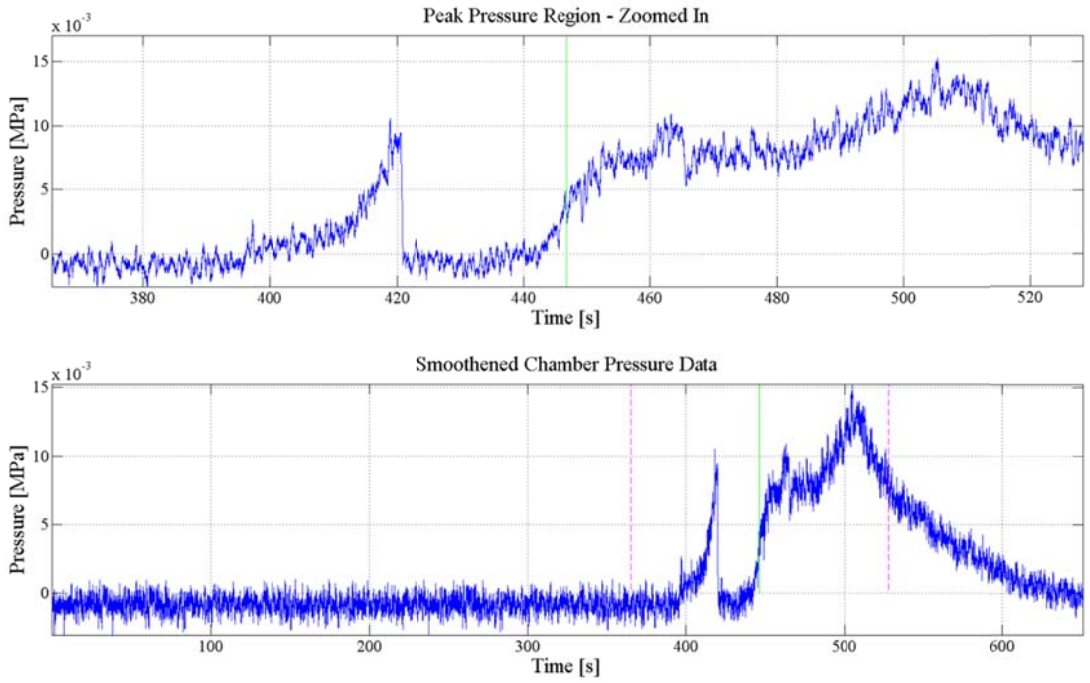

Figure 38. Internal Pressure Readings of Test Item 4

According to the visualization of test video recording and inspection of audio recordings, flame starts to come out of ventilation hole 177 seconds after the first ignition of fuel.

5.1.5. Test 5

Test item 5 is a short version of two types. It has a ventilation hole diameter of 8 mm. It has a 1 mm of thermoplastic liner between the explosive and the casing. Test item is shown in Figure 39.

Figure 39. Test Item 5 – Before the Test

According to the first inspection made after tests no deformation due to pressure or melting on the test item is observed as shown in Figure 40

Figure 40. Test Item 5 – After the Test

After the ignition of the fuel within the pool first increase in temperature is detected after 244 seconds of first data is recorded. This is accepted to be the reference time t_0 and other events detected during the tests will be referenced to this point.

Temperature measurements are given in Figure 41. Flame temperature readings are observed to be appropriate with STANAG 4240 requirements. As mentioned due to the lack of thermocouples no internal temperature measurements are taken in this test.

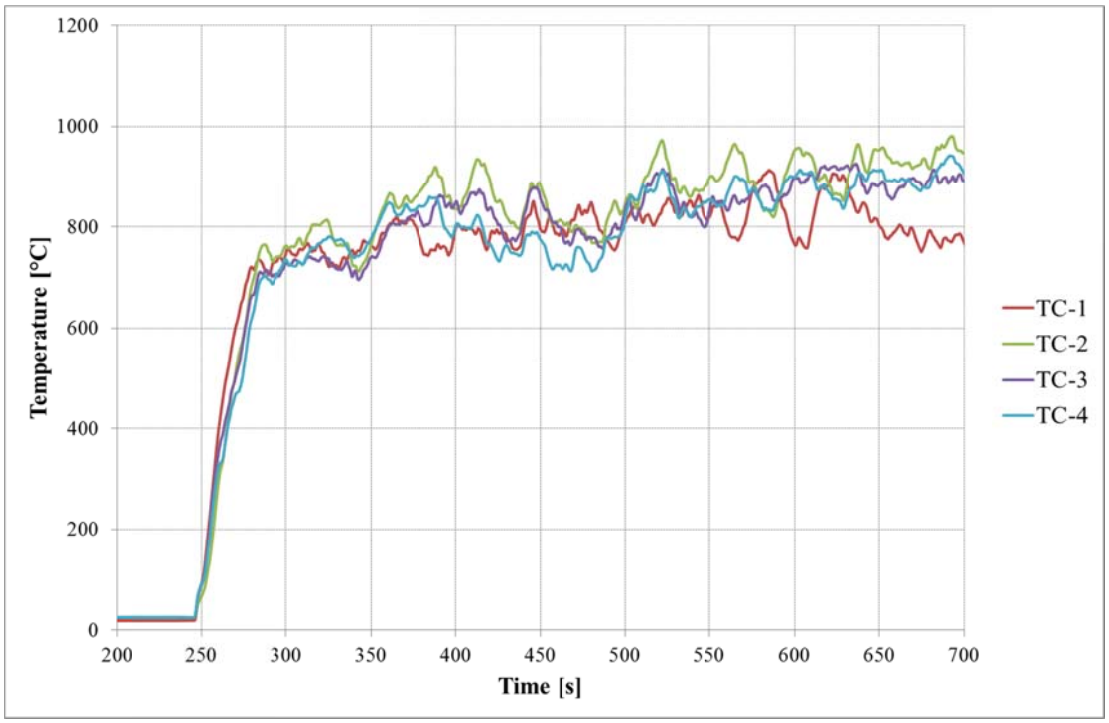

Figure 41. Flame and Internal Temperature Readings of Test Item 5

Chamber pressure readings given in Figure 42 indicate that pressure within the chamber starts to increase at t_0+106s. Pressure than increases to an average value of 0.015 MPa and reaches to a peak value of 0.032 MPa. It is observed that there is a pressure loss during the explosive burn at t_0+138s. This is considered to be because of ventilation plug debris removal from the ventilation hole.

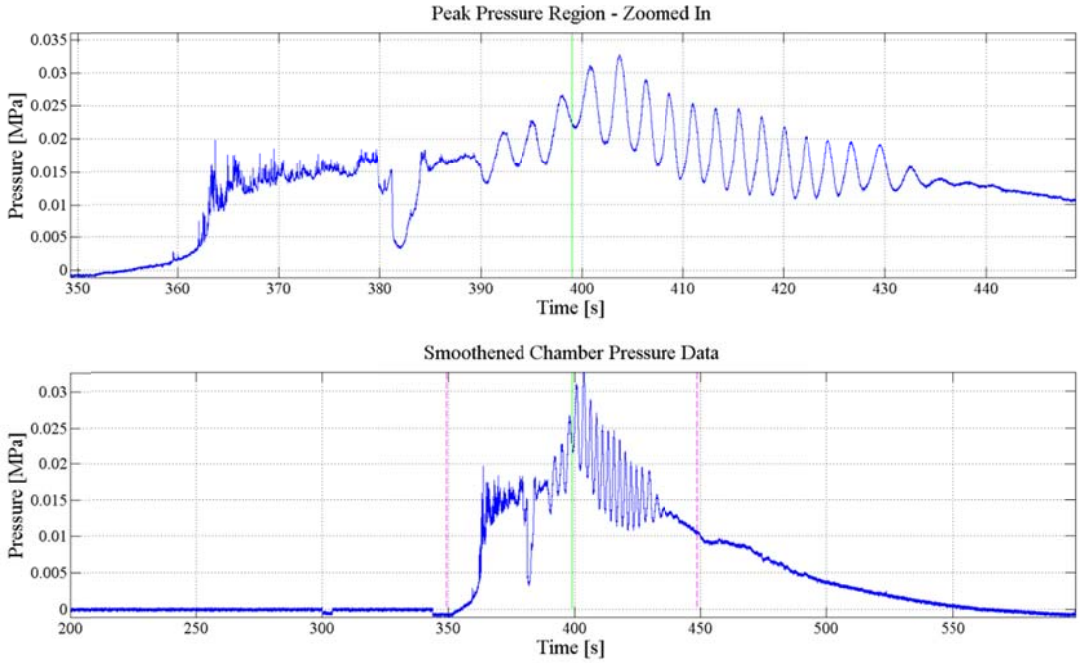

Figure 42. Internal Pressure Readings of Test Item 5

According to the visualization of test video recording and inspection of audio recordings, flame starts to come out of ventilation hole 106 seconds after the first ignition of fuel.

5.1.6. Test 6

Test item 6 is a long version of two types. It has a ventilation hole diameter of 6.85 mm. It has a 1 mm of thermoplastic liner between the explosive and the casing. Test item is shown in Figure 43.

Figure 43. Test Item 6 – Before the Test

According to the first inspection made after the test, deformation on the sidewall of the test item due to pressure or melting is observed as shown in Figure 44.

Figure 44. Test Item 6 – After the Test

After the ignition of the fuel within the pool first increase in temperature is detected after 314 seconds of first data is recorded. This is accepted to be the reference time t_0 and other events detected during the tests will be refereced to this point.

Temperature measurements are given in Figure 45. Flame temperature readings are observed to be appropriate with STANAG 4240 requirements.

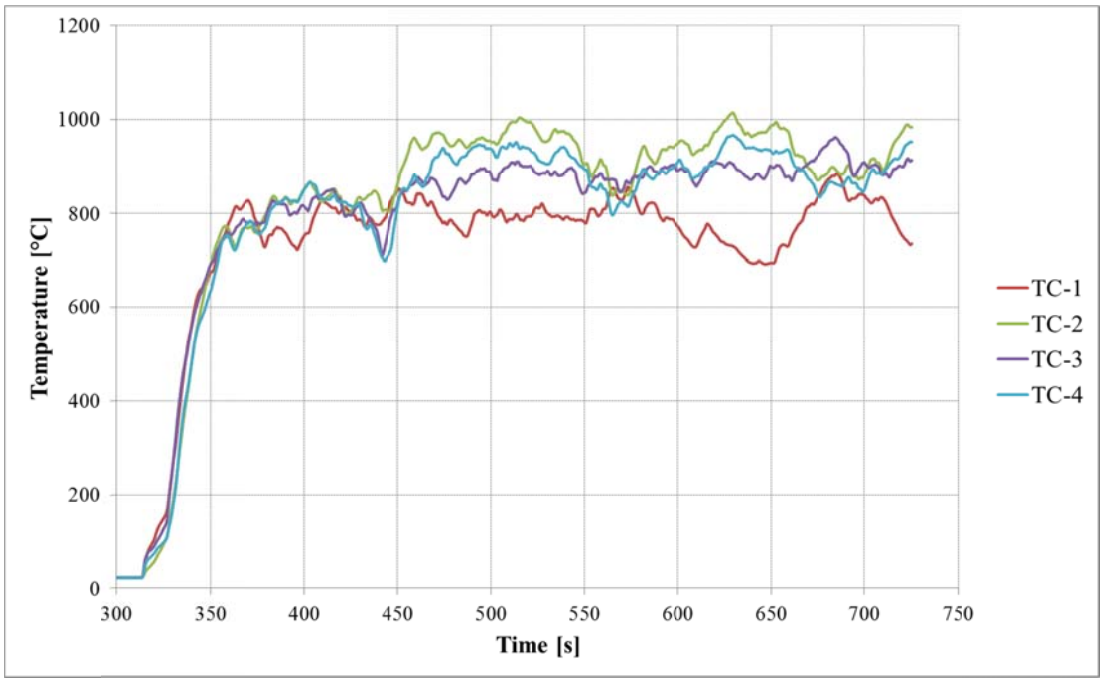

Figure 45. Flame and Internal Temperature Readings of Test Item 6

Chamber pressure readings given in Figure 46 indicate that pressure within the chamber starts to increase at t_0+95s. Pressure starts to drops at t_0+97s which is estimated due to the removal of ventilation plug debris from the ventilation hole. After that instance pressure starts to increase to a peak value of 0.35 MPa. The pressure drop after the peak values is reached is probably because of the torn apart sidewall of the test item. With the increased ventilation area, burn velocity of the explosive is considered to decrease.

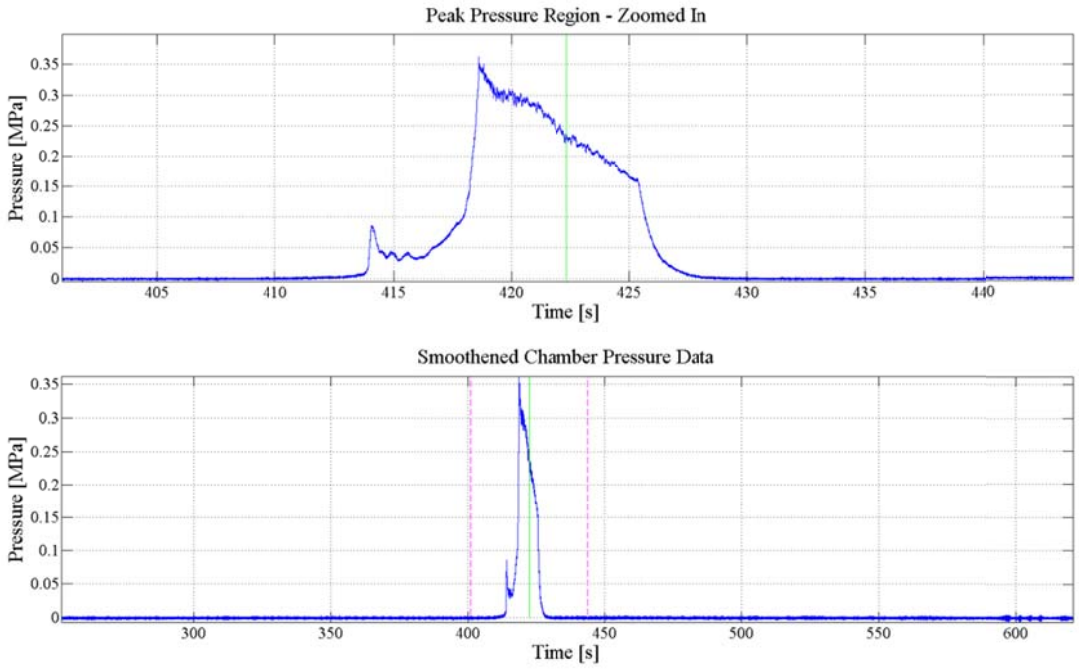

Figure 46. Internal Pressure Readings of Test Item 6

According to the visualization of test video recording and inspection of audio recordings, flame starts to come out of ventilation hole 95 seconds after the first ignition of fuel.

5.1.7. Test 7

Test item 1 is a long version of two types. It has a ventilation hole diameter of 6.85 mm. It has a 1 mm of HTPB liner between the explosive and the casing. Test item is shown in Figure 47.

Figure 47. Test Item 7 – Before the Test

According to the first inspection made after the test, deformation on the sidewall of the test item due to pressure or melting is observed as shown in Figure 48.

Figure 48. . Test Item 7 – After the Test

After the ignition of the fuel within the pool first increase in temperature is detected after 240 seconds of first data is recorded. This is accepted to be the reference time t_0 and other events detected during the tests will be referenced to this point.

Temperature measurements are given in Figure 49. No useful data could be obtained from the 4th thermocouple. But still it is possible to accept that flame temperature readings are observed to be appropriate with STANAG 4240 requirements.

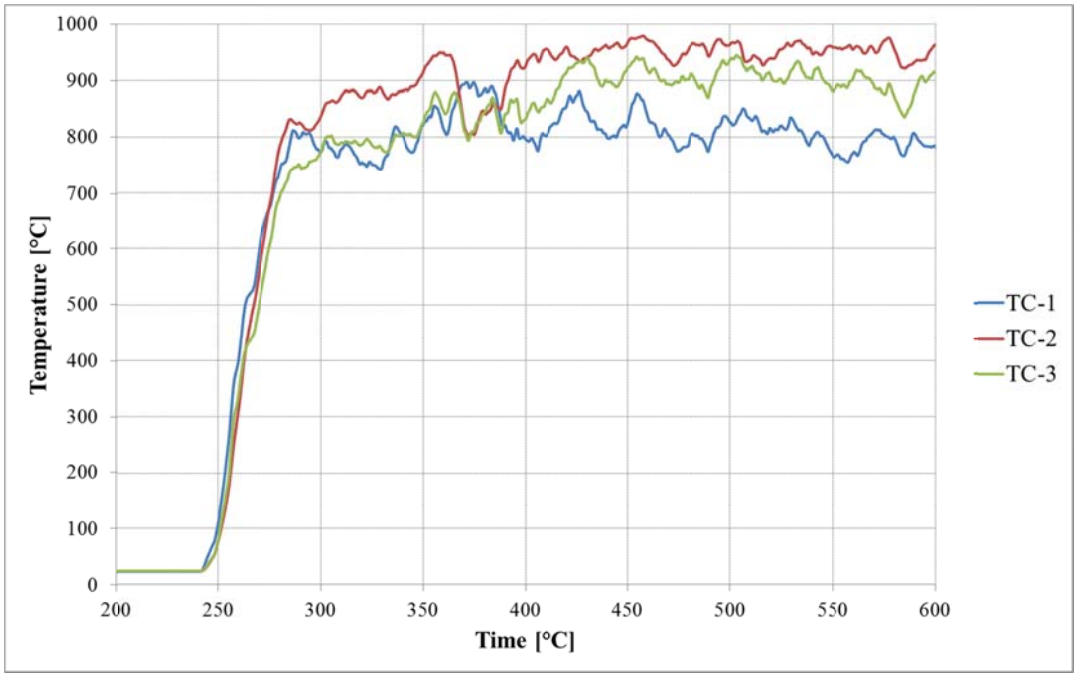

Figure 49. Flame and Internal Temperature Readings of Test Item 7

Chamber pressure readings given in Figure 50 indicate that pressure within the chamber starts to increase at t_0+107s and suddenly drops to "zero" at t_0+108s. The first pressure drop is considered to be the removal of the ventilation plug debris from the ventilation hole. After that pressure starts to increase at t_0+116s. Pressure increases to a value of 1.7 MPa and rapidly decreases afterwards. This second decrease is considered to be due to the torn apart side wall of the test item. Unfortunately, pressure starts to increase again at t_0+129s. This is accepted to be an evidence of second hole is still not enough to sustain the pressure low in the chamber. Thus, pressure starts to increase till the second vent hole enlarges or third and smaller ventilation hole is formed.

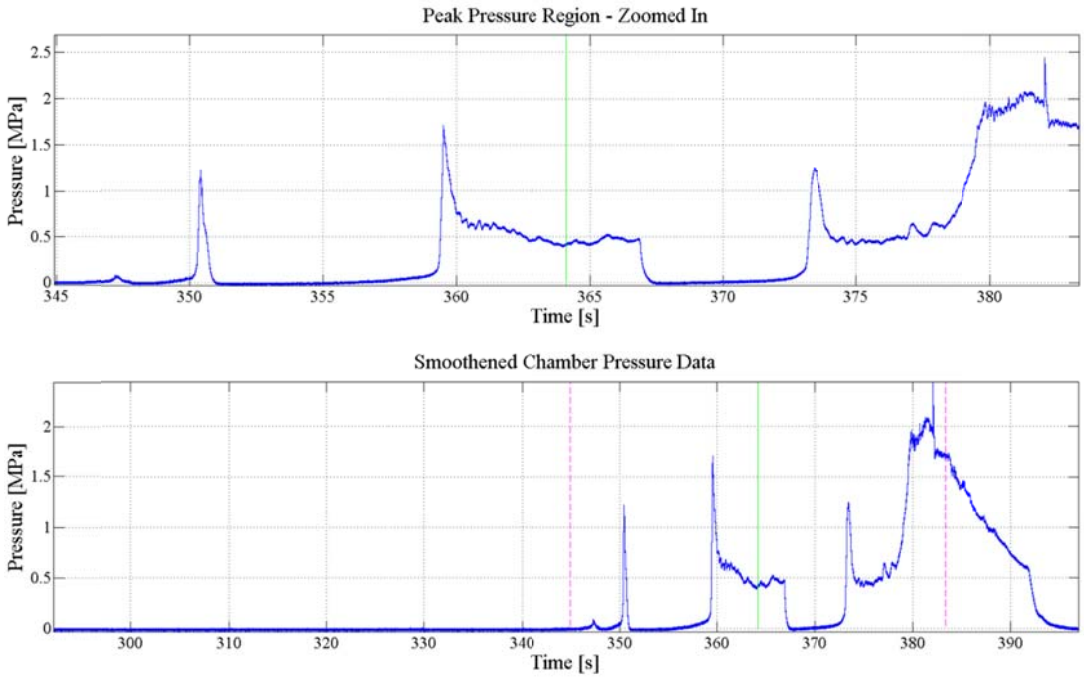

Figure 50. Internal Pressure Readings of Test Item 7

According to the visualization of test video recording and inspection of audio recordings, flame starts to come out of ventilation hole at t_0+107s.

Figure 51. Deflagration of PBXN-109 Explosive, Test 7

According to the visualization of test video recording and inspection of audio recordings, flame starts to come out of ventilation hole 107 seconds after the first ignition of fuel.

5.1.8. Test 8

Test item 1 is a long version of two types. It has a ventilation hole diameter of 7.1 mm. It has a 1 mm of HTPB liner between the explosive and the casing. Test item is shown in Figure 52.

Figure 52. Test Item 8 – Before the Test

According to the first inspection made after tests no deformation due to pressure or melting on the test item is observed as shown in Figure 53.

Figure 53. Test Item 8 – After the Test

After the ignition of the fuel within the pool first increase in temperature is detected after 76 seconds of first data is recorded. This is accepted to be the reference time t_0 and other events detected during the tests will be referenced to this point.

Temperature measurements are given in Figure 54. Temperature measurements are given in Figure 32. Flame temperature readings are observed to be appropriate with STANAG 4240 requirements.

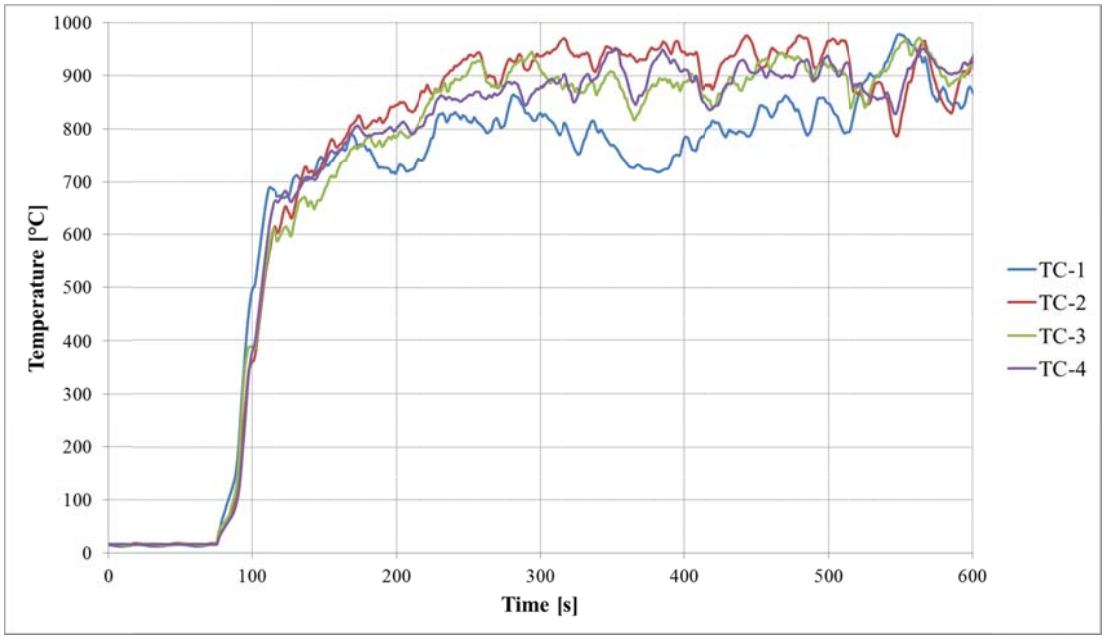

Figure 54. Flame and Internal Temperature Readings of Test Item 8

Chamber pressure readings given in Figure 55 indicate that pressure within the chamber starts to increase at t_0+114s and suddenly drops to "zero" at t_0+116s. Increase of pressure is considered to be the ignition of the explosive whereas sudden drop indicates the removal of ventilation plug debris.

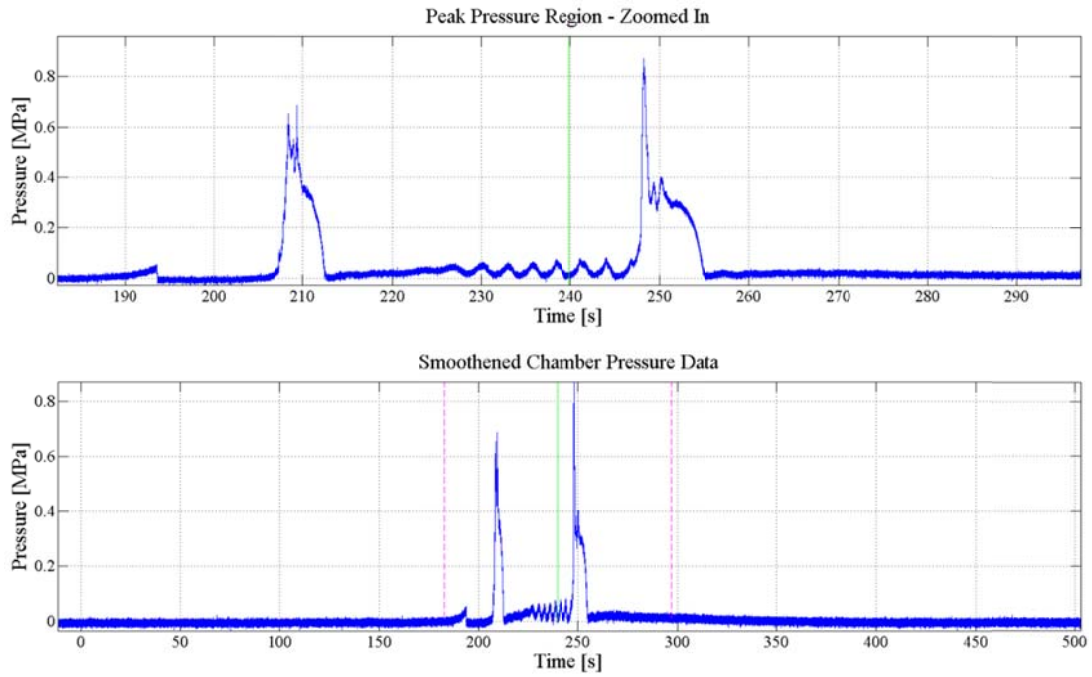

Figure 55. Internal Pressure Readings of Test Item 8

According to the visualization of test video recording and inspection of audio recordings, flame starts to come out of ventilation hole 114 seconds after the first ignition of fuel.

5.2. Comparison of Tests and Analyses

5.2.1. Determination of "True" Boundary Condition

Flame temperature measurements that have been made around the first test item are used to simulate boundary condition of the test item model in ANSYS Fluent. This is done by averaging the flame temperature over the entire event. Afterwards, 3 piecewise high order polynomial curves are fitted (Figure 56) along four different time ranges ($t \in [0,33.1s)$, $t \in [33.1s,71.1s)$, $t \in [71.1s,130.2s)$ and $t \geq 130.2s$). These curves are used as an input parameter for free stream temperature and external radiation temperature.

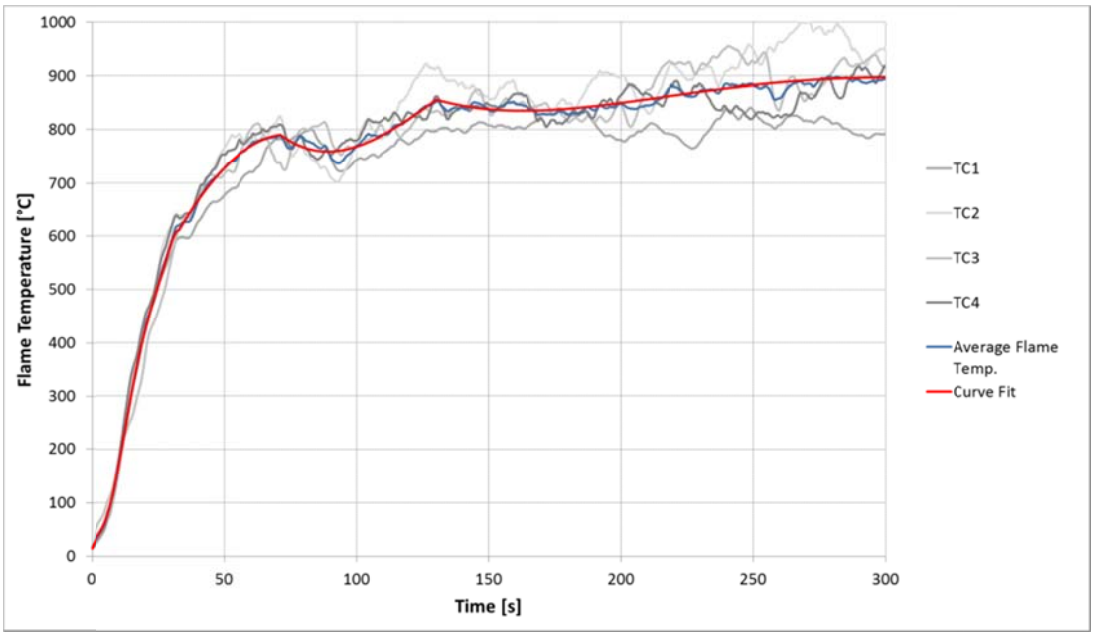

Figure 56. Flame Temperature Readings from the 1st Test

Temperature measurements that are taken both from front side surface and rear side surface are also averaged to check if the boundary condition that is implemented to the analysis represents these measurements. Both measurements and averaged temperatures are given in Figure 57.

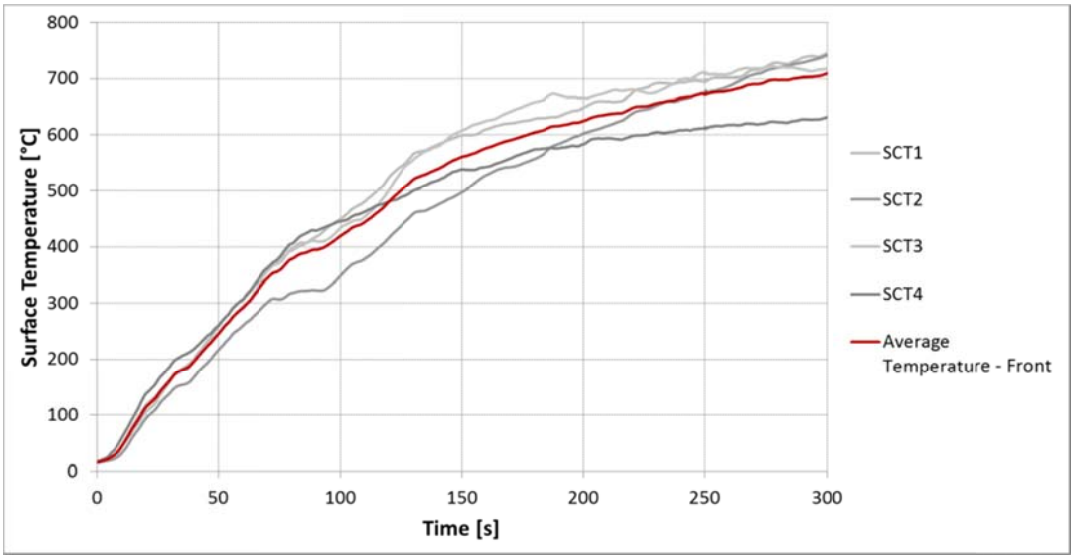

(a)

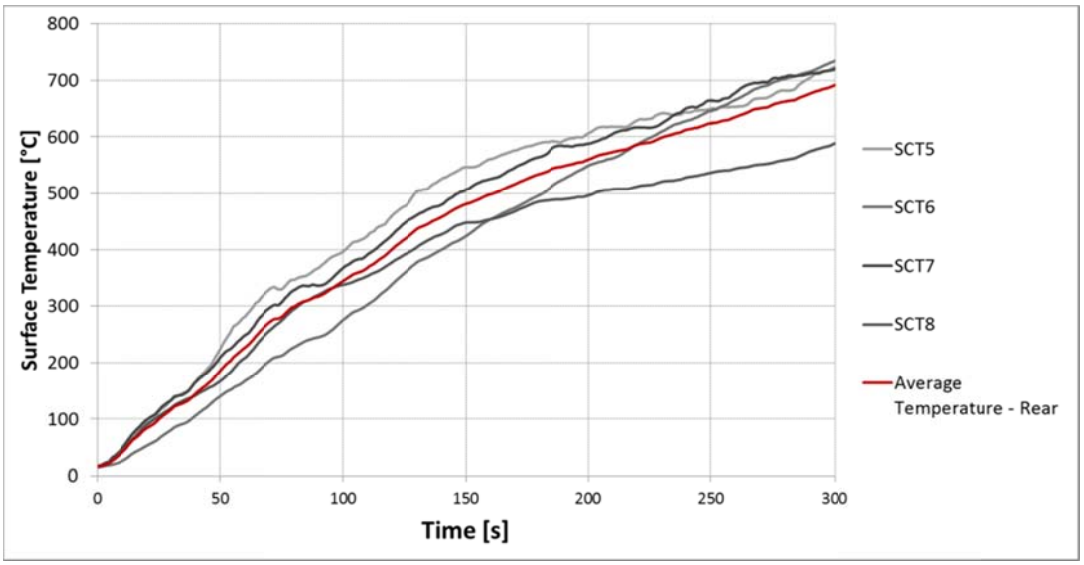

(b)

Figure 57. (a) Front Side, (b) Rear Side Surface Temperature Readings from the 1st Test Item

After the analyses of the first test item, surface temperatures from the analysis are compared with the test measurements. According to the comparison inconsistent results between test and analysis are observed as it can be seen in Figure 58.

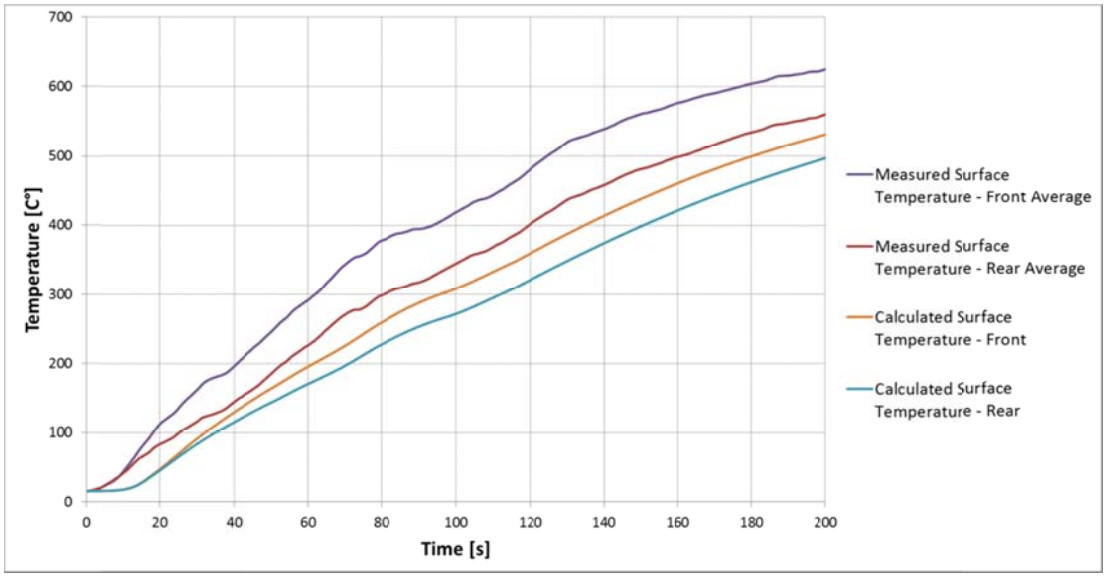

Figure 58 Initial Numerical Results of Test Flame Temperature Compared with Test Surface Temperatures

From the results, it is obvious that defined thermal boundary condition is not able to represent real heat transfer applied to the test item during the test. Although the common sense is to use durable, long lasting thermocouples for the application of measuring flame temperature, the error of the measurement is directly related to the type of the thermocouple choice. Reasons of measurement error are well concluded by Shannon and Butler [43]. Most errors associated with the use of thermocouples are due to the temperature between sensor and surrounding medium. When placed in the environments with high intensity like fires, thermocouples are tend to sense temperatures significantly different than the actual temperature of the medium of interest [44]. These errors are attributed to variations in the rate of energy transfer to and from the TC bead, temperature variations along the lead wires, and catalytic reactions between the metals comprising the bead at the surrounding gases.

Beside instantaneous temperature measurement error of the thermocouple, a delay between temperature increases in the very beginning of the test is also observed. This is also commented in Shannon and Butler's work [43] as this delay is because of the time required to transfer energy to the center of the thermocouple bead when being heated. The greater the mass of the thermocouple leads the greater the lag time between the thermocouple and actual gas temperature.

In our applications, 3mm thick thermocouples are used (ORDEL KTTE3x0.50 Ö 5K) for both gas and surface temperature measurements as survivability along the test is necessary as indicated in NATO publication [42], [5]. Otherwise, failure of a temperature sensor might lead to repetition of a test.

As it is not possible to use temperature data directly in the analyses as boundary condition, flame temperature has been tuned to satisfy the surface temperature readings that are taken from the first test and obtained from the analyses. Tuned flame temperature data is given in Figure 59.

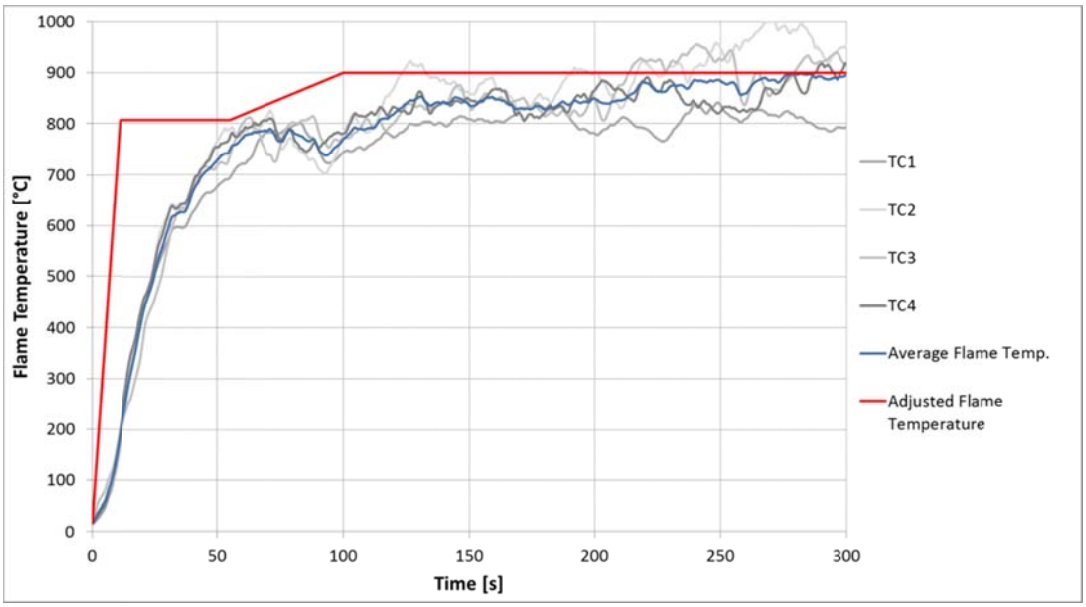

Figure 59 Tuned and Simplified Flame Temperature Distribution

After analyzing different simplified flame temperature distributions as a model, the curve shown in Figure 60 is obtained from Fluent which successfully matches with the test temperature measurements.

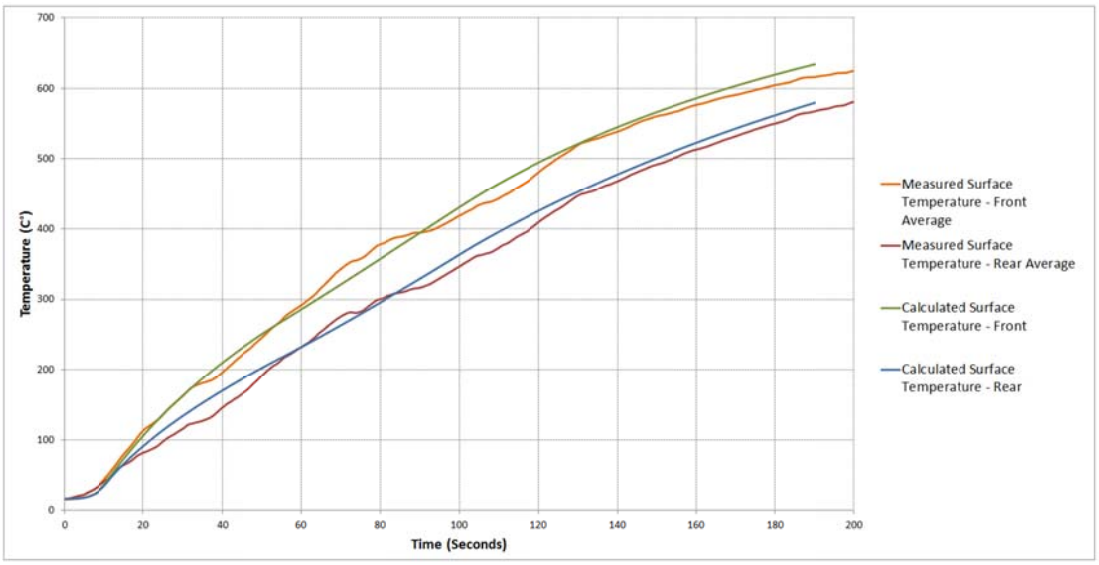

Figure 60. Surface Temperature Comparison of Test and Numerical Results - Test Case 1

Corrected and simplified temperature boundary condition is applied for the further analyses.

5.2.2. Computation Results for Time to Reaction Analyses and Comparison of the Results with Test Results

After the first analyses, it is concluded that the effect of buoyancy is below 1% when TtR values are compared. Thus, further analyses are carried out with the 2-D axisymmetric approach. Internal parts are not modeled in axisymmetric simulations. Time step and element size dependency of the analyze model is checked as shown in Table 3 and Table 4 and tuned as the effect of both element size and time step will not affect the result by more than 0.1%.

Table 3. Mesh Refinement Study

Run Type	Max Element Size	Number of Elements	TtR [s]	Difference with Fine Mesh (%)
Fine Mesh	0.0005	49334	189.7	0.00
Medium Mesh	0.001	12724	190.6	0.47
Coarse Mesh	0.002	3407	196.4	3.53

Table 4. Time Refinement Study

Run Number	Time Step Size	TtR	Difference with 1st Run (%)
1	0.1	189.7	0.00
2	0.2	189.6	0.05
3	0.3	188.9	0.42
4	1	188	0.90
5	2	186	1.95
6	10	180	5.11

Total of 49334 elements in 2-D are used whereas 1654200 elements are used in 3-D version of the analyses. Both mesh construction and temperature gradients of test item containing 1 mm of HTPB liner (for test cases 7-8) are shown in Figure 61.

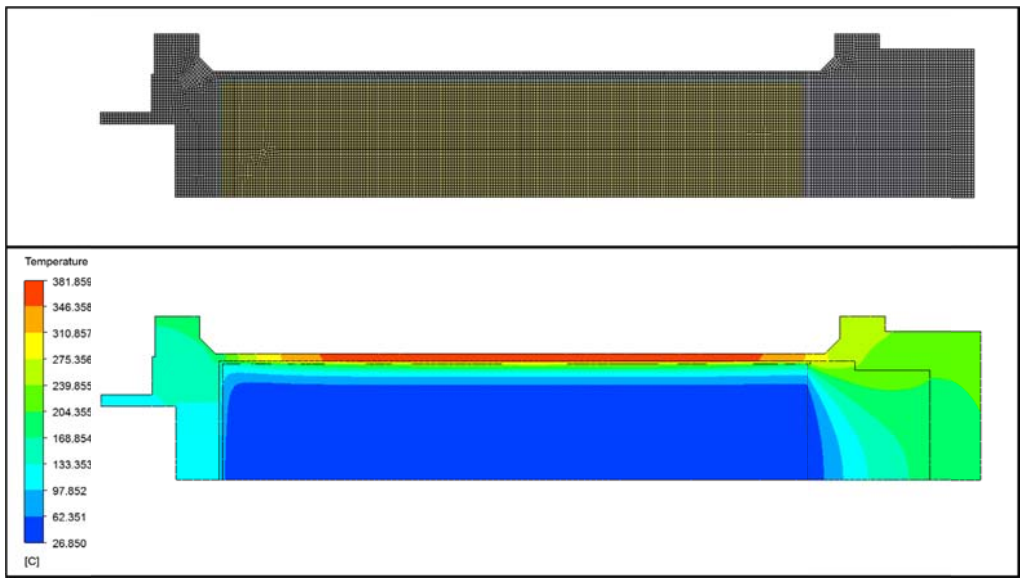

Figure 61. Mesh Distribution (top) and Temperature Gradient (bottom) of Test Items 7-8

Ignition can be detected by tracking the maximum temperature plot over the explosive volume. As specified above, heat generation is a function of temperature (Eq. 4) that is implemented into the Fluent by UDF tool. If temperature of a cell rises above the critical temperature, which is in this case ~220°C for PBXN-109, heat generated is converged to infinite so does the temperature (Figure 62).

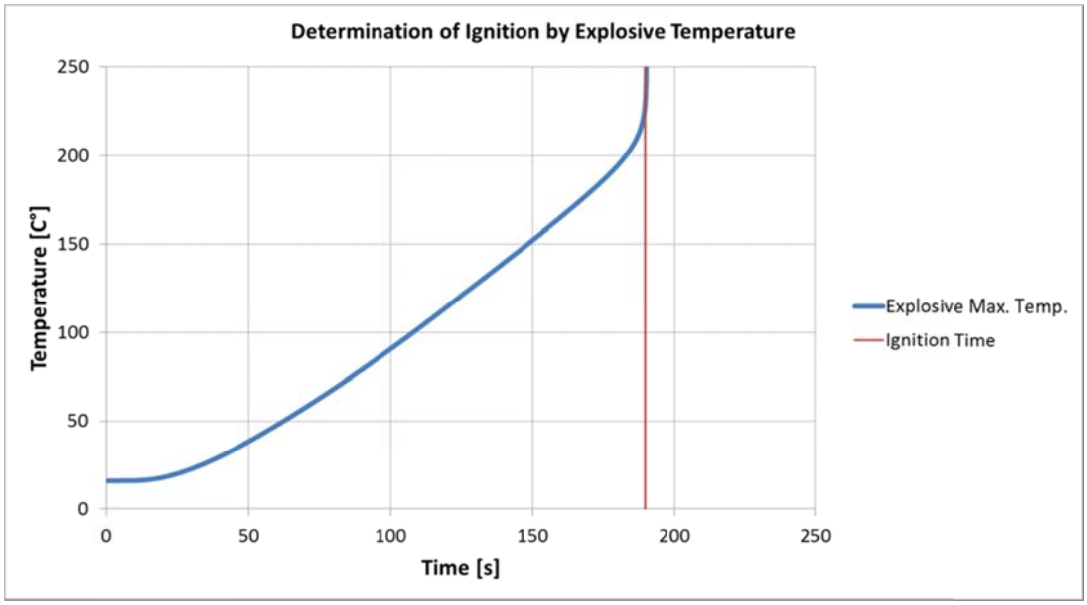

Figure 62. Maximum Temperature Plot of the Explosive and Ignition Time

Results are given for fine mesh since computation time is low in an 8 core Intel Xeon CPU X5650 @ 2.67GHz (2 processors) computer.

Summary of the test configurations and comparison of calculated and observed time to reaction are given in Table 5.

Table 5. Comparison of Calculated and Observed TtR

Test Item No	Explosive L/D	Liner Thickness [mm]	Liner Type	Predicted TtR [s]	Observed TtR [s]	Difference [s]	Error (Experiment - Numerical) %
1	2.67	3.50	HTPB Based Thermoset	189.7	200	-10.3	-5.2
2	1.71	3.50	Thermoplastic Liner	179.7	172	7.7	4.5
3	1.71	3.50	Thermoplastic Liner	179.7	178	1.7	1.0
4	1.71	3.50	Thermoplastic Liner	179.7	177	2.7	1.5
5	1.60	1.00	Thermoplastic Liner	98.8	106	-7.2	-6.8
6	1.60	1.00	Thermoplastic Liner	98.8	95	3.8	4.0
7	1.60	1.00	HTPB Based Thermoset	103.8	107	-3.2	-3.0
8	1.60	1.00	HTPB Based Thermoset	103.8	114	-10.2	-8.9

The largest difference between the predicted and observed ignition times occurred with 8.9 percent difference for 8 tests. Addressing the 8.9% difference, the prediction does not take into account the decomposition/melting of the liner and decomposition of the explosive that occurs before ignition in the analyses. It is assumed that the liner thickness is constant along the solution. These phase shifting and/or chemical reactions are thought to effect heat transfer to explosive through the test item hence increasing the error.

Another source of the error is the unavailability of simulating the variation of temperature in medium hence on the test item. Flame temperature may directionally vary within the hearth either caused by wind or the chaotic environment of its nature. as shown in Figure 56 different thermocouples have different temperature readings. The temperature distribution between thermocouples is shown in Figure 57. As mentioned above, the average of all 4 thermocouples is used as a temperature boundary condition. On the other hand, because of directionality of the flame, heat flux on one surface might be higher than the other three causing a hot spot along the circular direction. Thus, even if by small amounts we are already expecting to have different ignition times for the test item having the same geometry and liner

type/thickness. Even with these limitations, predicted ignition time can be accepted to be close to the experimental data.

5.2.3. Computation Results for Time to Reaction Analyses and Comparison with Test Results

Determination of ventilation characteristic of the system, pressure readings from each test is obtained. Unfortunately, as the test item is designed to have low fragmentation impact upon explosion due to instantaneous pressure built up within the chamber, some of the test items above 0.7MPa are observed to be torn. Therefore, pressures above this are interpreted to be much higher than what is measured. Experimental results are compared with the numerical results obtained from dimensionless MATLAB Simulink code. Sample output data of an test item having a Ø9 mm of ventilation hole is given in Figure 63. Burn reaction is assumed to spread all over the explosive surface as there are no inhibitor line is used like the applications in rocket motors. Because of that, initial burn area in calculations is taken as total burn area of the explosive.

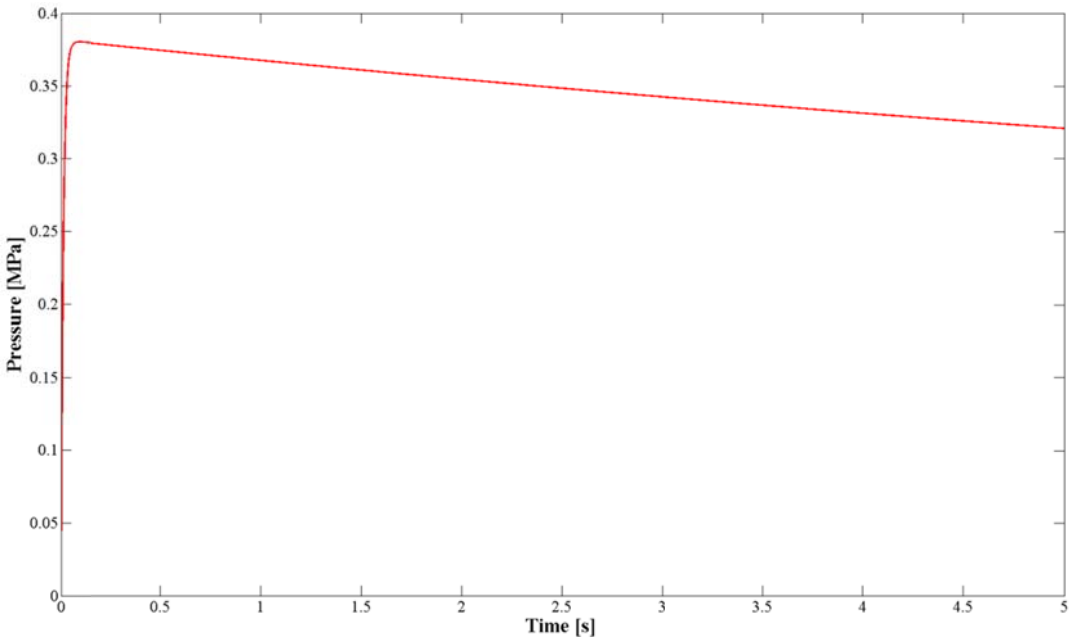

Figure 63. Sample MATLAB Simulink Output, Test Item with Ø9mm Vent

As there are different test items having different amount of explosive, results are given as the ratio of ventilation area over total explosive area in Figure 64 (A_{vent}/A_{burn}).

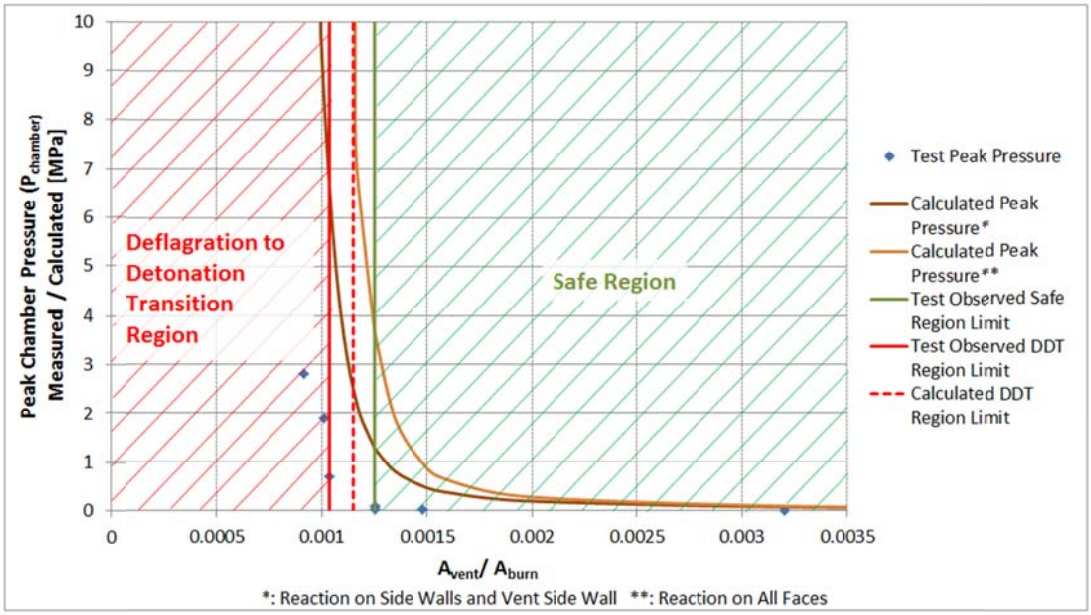

Figure 64. Comparison of Experimental and Numerical Results of Peak Pressure

Looking at the graph of pressure change with ventilation area, it is hard to say where deflagration to detonation transition (DDT) will occur or where the safe side is. But having experienced that the test items are torn above A_{vent}/A_{burn} of 0.00104 we have accepted that this is the limit for DDT. On the other hand, test items that have the smallest A_{vent}/A_{burn} are assumed to be the limit of safe region. Unknown region between the safe and DDT limits where there is no tests made can be expected to be unstable in an engineering point of view.

Numerical calculations of different scenarios predict having an A_{vent}/A_{burn} smaller than 0.00115 will cause chamber pressure to diverge and lead to DDT. Although numerical results predict using a slightly smaller ventilation area, reasons behind this is predictable. Burn area is taken to be the whole explosive area initially. Although this is acceptable for a critical design methodology, the real case might not be so especially for low burn rates. The reason that numerical calculations show higher

peak pressures at higher A_{vent}/A_{burn} (> 0.00125) is probably because of extrapolated burn data between 0-2 MPa and burn surface area approximation.

CHAPTER 6

CONCLUSION AND FUTURE WORK

6.1. Conclusion

Total of 8 tests are examined in this study utilizing thermal modeling of liquid fuel fire. They are performed in order to observe ignition time of generic test items. From the first test, an improved temperature boundary condition is obtained. With the more realistic boundary condition, 4 different analyses are conducted for different test items with 2-D, axisymmetric approach. This is done since the 3-D model where the buoyancy terms are included does not change the predicted time by more than 1%.

Predicted ignition times and test results shows a maximum difference of 8.9%. Possible reasons of this error are discussed. An improvement on the methodology can be made upon implementing a melting and/or decomposition model into the ANSYS Fluent. By considering the current results methodology, using a 2-D axisymmetric thermal analysis for predicting the time to reaction seems to be applicable.

Ventilation characteristic of a system that contains an explosive of type PBXN-109 is also studied. For this purpose, burn characteristics under relatively low pressures (0-10 MPa) are obtained using a strand burner test setup. Next, this data is used within the self-developed dimensionless code to calculate the critical ventilation area and compared with the experimental data. According to the comparison made, results show some discrepancies at 10.9%. Possible reasons for the prediction of critical ventilation area are also discussed in the previous section.

By this work, it will be possible for one to predict the ignition time of a munition containing an energetic material by knowing the heat generation characteristic of that energetic material by using the ANSYS Fluent or any other software that is eligible to model the heat transfer. By doing so, it will be also possible to study critical

thermal path of the energetic system and take necessary precautions to avoid any violent reactions.

Another benefit of this work is that, it will guide a designer to design ventilation mechanism that will allow venting the system safely where the explosive will not lead to deflagration to detonation transition.

6.2. Future Work

A methodology for a design phase of an insensitive munition is discussed in this study. Although the methodology is valid for all solid type energetic materials, the current study only covers an explosive named PBXN-109. Further studies can be made for other type of explosives.

To improve the accuracy of the time to reaction analyses, melting and decomposition of the liner and explosive can be implemented by complex user defined functions and other tools. However, before proceeding with modeling studies detailed physics behind this should be understood and several tests should be made.

Despite a methodology to understand and improve the way energetic material acts under thermal stimuli, a coupled thermal, chemical and mechanical solver can be developed. However, it is obvious that this will require a huge amount of effort.

REFERENCES

[1] Proud G. W., *Ignition and Detonation in Energetic Materials: An Introduction*, STO-EN-AVT-214 Lecture Series September 2013.

[2] *STANAG 4439 JAIS (Edition 3) – Policy for Introduction and Assessment of Insensitive Munitions*, 17 March 2010.

[3] Banton, R., *Model Development for Insensitive Munitions (IM) Simulations*, U.S. Army Research Laboratory, 2006.

[4] *NATO Allied Ordnance Publication (AOP) 39, Edition 3, Guidance on the Assessment and Development of Insensitive Munition*, March 2010.

[5] Zukas, A.Z., Walters, P.W., Ed., *Explosive Effects and Applications*, Springer-Verlag New York Inc., New York, USA, 1998.

[6] Lee, P.R., *Course Notes on Initiation and Mechanical Properties of Energetic Materials and Their Influence on Insensitive Munitions (IM) Design*, Computational Mechanics Associates, Baltimore, USA, 2005.

[7] Desailly, D., Guengant, *Y., Numerical Simulation of Reaction Violence to Cook-off Experiments*, NDIA Insensitive Munitions and Energetic Materials Symposium, Orlando, USA, 2003.

[8] Roger L. S., *Lecture Notes on AVT-214, Approach to IM Policy – Defining the Need*, STO-EN-AVT-214 Lecture Series September 2013.

[9] Hayles, D.R., *How Safe Should Our Weapons Be?* Maxwell Air Force Base, Alabama, USA, 2005.

[10] White, A., Parker, R.P., *Cost-Benefit Analysis Concept for Insensitive Munitions Policy Implementation*, DSTO Aeronautical and Maritime Research Laboratory, Australia, 1999.

[11] Doherty, R., Watt, D., *Insensitive Munitions-Coming of Age,* International Annual Conference – ICT, Fraunhofer Institut Für Chemische Technologie, Germany, 1999.

[12] Isler, J., *The Transition to Insensitive Munitions*, Propellants, Explosives, Pyrotechnics, Vol.23, p.283-291, 1998.

[13] Victor A.C., *Simple Calculation Methods for Munitions Cook-Off Times and Temperatures*, Propellants, Explosives, Pyrotechnics, Vol. 20, pp. 252-259, 1995.

[14] Aydemir, E., Ulas, A., Serin, N., *Reacon-1D: Thermal Analysis Code for Energetic Materials Using Finite Element Method*, New Trends in Research of Energetic Materials, Pardubice, Czech Republic, 2007.

[15] Semenov, N.N., *Z. Phys.*, Vol. 48, p. 571, 1928.

[16] Frank-Kamenetskii, D.A., *Acta Physiochim, URSS*, Vol.10, p. 365, 1939.

[17] Zinn, J., Mader, C.L. *Thermal Initiation of Explosives, J. Appl. Phys., Vol. 31(2), p. 323*, 1960.

[18] Merzhanov, A.G., Abramov, V.G., *Propellants, Explosives and Pyrotechnics*, Vol. 6, p. 130, 1981.

[19] Sućeska, M., *A Computer Program Based on Finite Difference Method for Studying Thermal Initiation of Explosives*, J. Thermal Analysis and Calorimetry, Vol. 68, p 865-875, 2002.

[20] Anderson, C.A., *TEPLO – A Heat Conduction Code for Studying Thermal Explosion in Laminar Composites*, Los Alamos Scientific Laboratory, LA-4511, Los Alamos, USA, 1970.

[21] Isler, J., Kayser, D., *Correlation between Kinetic Properties and Self-Ignition of Nitrocellulose*, 6th Symp. Chem. Probl. Connected Stab. Explos, Kungalav, Sweden, 1982.

[22] McGuire, R.R., Tarver, C.M., *Chemical Decomposition Models for Thermal Explosion of Confined HMX, RDX, and TNT Explosives*, Lawrence Livermore Laboratory, UCRL-84986, Livermore, USA, 1981.

[23] Pakulak J. M., *Simple Techniques for Predicting Sympathetic Detonation and Fast and Slow Cookoff Reaction of Munitions*, Technical Report, Naval Weapons Center, June 1988.

[24] Nichols, A.L., Anderson, A., Neely, R., Wallin, B, *A Model For High Explosive Cookoff*, 12th International Detonation Symposium, 2002.

[25] McClelland, M.A., Maienschein, J. L., Nichols, A.L., Wardell, J.F., Atwood, A.I., Curran, P.O., *ALE3D Model Predications and Materials Characterization for The Cookoff Response of PBXN-109*, 20th Propulsion Systems Hazards Subcommittee, 2002.

[26] Kenneth J., Graham, Aerojet, Culpeper VA, *Mitigation of Fuel Fire Threat to Large Rocket Motors by Venting*, 2010 Insensitive Munitions & Energetic Materials Technology Symposium, Munich, Germany, 11-14 October 2010.

[27] Victor, A.C., *Cookoff Protocol for Munition Assessment*, Victor Technology, Ridgecrest, California, USA, 1994.

[28] Swierk T., *Fuel Fire Experts Working Group IV Meeting Summary*, September 2014.

[29] Yagla J., D. Griffiths, D. Hubble, K. Ford, E. Washburn, *Experimental Development of Propane Burners for Fast Cook Off Testing*, Insensitive Munition and Energetic Material Technology Symposium, October 2013.

[30] Pershing D. W., *Center for the Simulation of Accidental Fire and Explosion Annual Report*, September 1999.

[31] Luketa A, *Assessment of Simulation Predictions of Hydrocarbon Pool Fire Tests*, Fire and Aerosol Sciences Department Sandia National Laboratories, 2010.

[32] Rawat R., Pitsch H., and J. F. Ripoll, *Large-Eddy Simulation of Pool Fires with Detailed Chemistry Using an Unsteady Flamelet Model*, Center of Turbulence Research Proceeding of the Summer Program, 2002.

[33] Echeverria F., Bernardez P., Gonzalo R., *Use of CFD Modelling in The Design of a IM Warhead to Cook-Off Stimuli*, Insensitive Munition and Energetic Material Technology Symposium, May 2015.

[34] Ford K.P., Davis N.C., Farmer A.D., Washburn E.B, Atwood A.I., Wilson K.J., Abshire J.P., M.L. Shewmaker, Z.P. Goedert, C.J. Wheeler, P.O. Curran, J. Covino, *Subscale Fast Cookoff Test Result*, Insensitive Munition and Energetic Material Technology Symposium, 2010.

[35] *http://www.aerojet.engr.ucdavis.edu/fluenthelp/html/ug/node998.htm*, FLUENT 6.3 User's Guide, last access date: June 2015

[36] Anderson B. W. *The Analysis and Design of Pneumatic Systems*, Wiley, NY, 1967, p. 19.

[37] *http://www.grc.nasa.gov/WWW/CEAWeb*, last access date: June 2015.

[38] Maienschein J.L., Wardell J.F., Weese R.K., Cunningham B.J., Tran T.D, *Understanding and Predicting the Thermal Explosion Violence of HMX-Based and RDX-Based Explosives – Experimental Measurements of Material Properties and Reaction Violence*, 12th International Congerence Symposium, San Diego, California, August, 2002.

[39] Ulas A., Y.-C. Lu & Kenneth K. Kuo (2003) *Ignition and Combustion Characteristics of RDX-Based Pseudopropellants*, Combustion Science and Technology, 175:4, 695-720, DOI: 10.1080/00102200302391.

[40] Maienschein J.L., Wardell J.F., *Deflagration Behavior of PBXN-109 and Composition B at High Pressures and Temperatures*, Lawrance Livermore National Laboratory, March 11, 2002.

[41] Curdaneli S., *Experimental Analysis on the Measurement of Ballistic Properties of Solid Propellants*, M.Sc. thesis in Mechanical Engineering submitted to Middle East Technical University, Turkey, May 2007.

[42] NATO Standard 4240 (Edition 2), *NATO Liquid Fuel / External Fire, Munition Test Procedures*, April 2003.

[43] Shannon K.S., Butler B.W., *A Review of Error Associated with Thermocouple Temperature Measurement in Fire Environments, Second International Wildland Fire Ecology and Fire Management Congress and Fifth Symposium On Fire And Forest Meteorology*, November 2003

[44] Jones J.C., *On the Use of Metal Sheathed Thermocouples in a Hot Gas Layer Originating From a Room Fire. Journal of Fire Science*, 13, 257-260., 1995

APPENDIX A

MATLAB FUCNTIONS

Input.m

```
clear, clc, close all
Pi=0; % Pa, gauge pressure
ro=1670; % kg/m3
ri=0.039; % m, initial radius of the explosive
Li=0.125; % m, initial length of the explosive
Vi=9.3669E-005; % m3
T_chamber=2552.84; % K
R_chamber=339.28; % Pa.m3/kg/.K
k_chamber=1.2153;
Cd=0.82;
```

Explosive Geometry Calculation Function

```
function Ab  = Expo_Geo(ri,Li,d)
r=ri-d; % Remaining radius of the explosive
L=Li-2*d; % Remaining length of the explosive
if r<=0 || L<=0
   r=0;
   L=0;
end
Ab=(2*pi*(r^2)+2*pi*r*L); % Explosive burn area, based on the assumption that
burning takes places on all explosive surfaces
```

Burn Rate Calculation Function

```
function rb  = Burn_rate(p)
n1=0.93; % m/s - pascal
a1=1.223E-9; % m/s - pascal - Ref: SAGE curve fit, 0-10 MPa
n2=1.3196; % m/s - pascal
```

```
a2=2.90626E-12; % m/s - pascal - Ref: Livermore Lab., 0-10 MPa
if p<=10^7
  rb=a1*p^n1;
else
  rb=a2*p^n2;
end
```